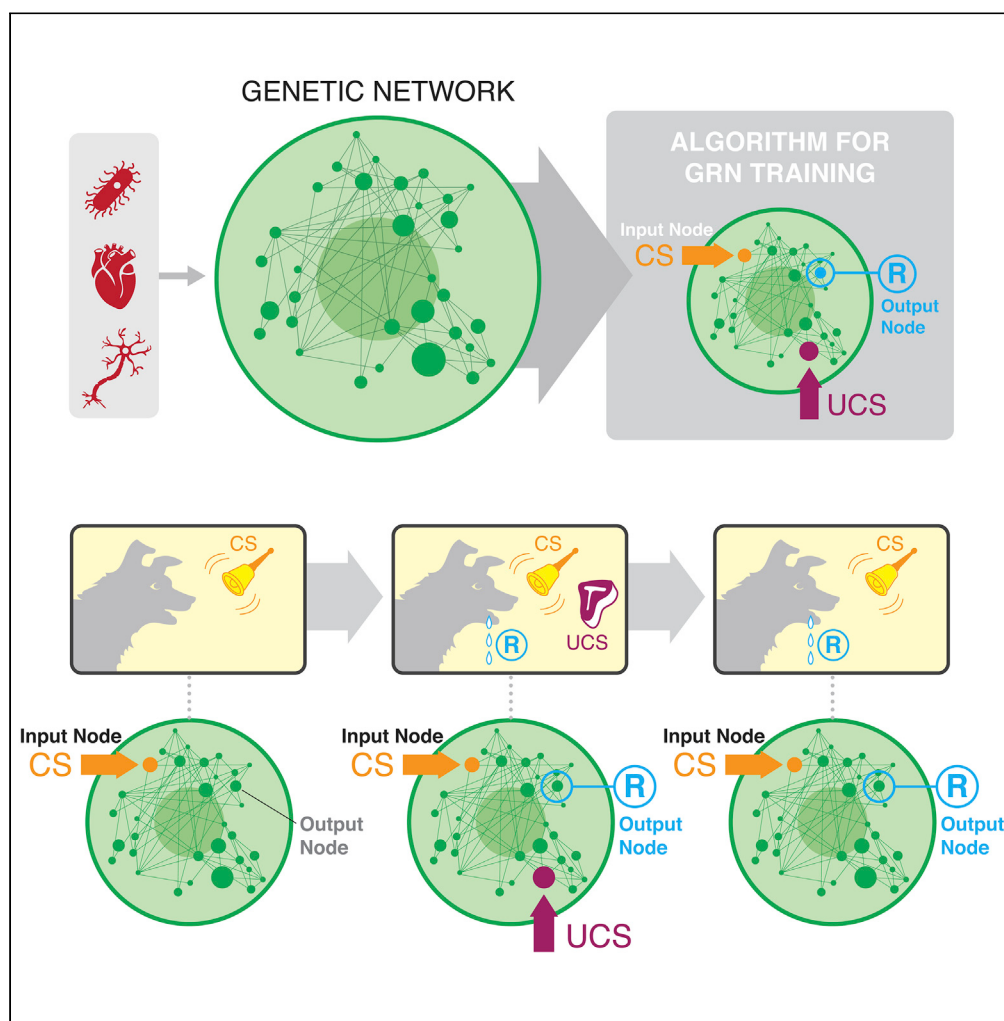


Article

Gene regulatory networks exhibit several kinds of memory: Quantification of memory in biological and random transcriptional networks



Surama Biswas,
Santosh Manicka,
Erik Hoel, Michael
Levin

michael.levin@tufts.edu

HIGHLIGHTS
Gene regulatory
networks' dynamics are
modified by transient
stimuli

GRNs have several
different types of memory,
including associative
conditioning

Evolution favored GRN
memory, and
differentiated cells have
the most memory capacity

Training GRNs offers a
novel biomedical strategy
not dependent on genetic
rewiring

Biswas et al., iScience 24,
102131
March 19, 2021 © 2021 The
Author(s).
<https://doi.org/10.1016/j.isci.2021.102131>



Article

Gene regulatory networks exhibit several kinds of memory: Quantification of memory in biological and random transcriptional networks

Surama Biswas,¹ Santosh Manicka,¹ Erik Hoel,¹ and Michael Levin^{1,2,3,*}

SUMMARY

Gene regulatory networks (GRNs) process important information in developmental biology and biomedicine. A key knowledge gap concerns how their responses change over time. Hypothesizing long-term changes of dynamics induced by transient prior events, we created a computational framework for defining and identifying diverse types of memory in candidate GRNs. We show that GRNs from a wide range of model systems are predicted to possess several types of memory, including Pavlovian conditioning. Associative memory offers an alternative strategy for the biomedical use of powerful drugs with undesirable side effects, and a novel approach to understanding the variability and time-dependent changes of drug action. We find evidence of natural selection favoring GRN memory. Vertebrate GRNs overall exhibit more memory than invertebrate GRNs, and memory is most prevalent in differentiated metazoan cell networks compared with undifferentiated cells. Timed stimuli are a powerful alternative for biomedical control of complex *in vivo* dynamics without genomic editing or transgenes.

INTRODUCTION

Gene regulatory networks (GRNs) are key drivers of embryogenesis, and their importance for guiding cell behavior and physiology persists through all stages of life (Alvarez-Buylla et al., 2008; Huang et al., 2005). Understanding the dynamics of GRNs is of high priority not only for the study of developmental biology (Davidson, 2010; Peter and Davidson, 2011) but also for the prediction and management of numerous disease states (Fazilitay et al., 2019; Qin et al., 2019; Singh et al., 2018). Much work has gone into the computational inference of GRN models (De Jong, 2002; Delgado and Gómez-Vela, 2019), and the development of algorithms for predicting their dynamics over time (Schlitt and Brazma, 2007). However, the field has been largely focused on rewiring—modifying the inductive and repressive relationships between genes—to control outcome. This can be difficult to control in biomedical contexts, and even in amenable model systems, it is often unclear what aspects of the network should be altered to result in desired system-level behavior of the network. Dynamical systems approaches have made great strides in understanding how GRNs settle on specific stable states (Herrera-Delgado et al., 2018; Zagorski et al., 2017). However, significant knowledge gaps remain concerning temporal changes in GRN dynamics, their plasticity, and the ways in which their behavior could be controlled for specific outcomes via inputs not requiring rewiring.

Thus, an important challenge in developmental biology, synthetic biology, and biomedicine is the identification of novel methods to control GRN dynamics without transgenes or genomic editing, and without having to solve the difficult inverse problem (Lobo et al., 2014) of inferring how to reach desired system-level states by manipulating individual node relationships. A view of GRNs as a computational system, which converts activation levels of certain genes (inputs) to those of effector genes (outputs), with layers of other nodes between them, suggests an alternative strategy: to control network behavior via inputs—spatiotemporally regulated patterns of stimuli that could remodel the landscape of attractors corresponding to a system’s “memory.” A broad class of systems, from molecular networks (Szabó et al., 2012) to physiological networks in somatic organs (Goel and Mehta, 2013; Turner et al., 2002), exhibit plasticity and history-based remodeling of stable dynamical states. Could GRNs likewise exhibit history dependence that could help us explain the variability of cellular responses, and that could be exploited to control their

¹Allen Discovery Center, Tufts University, Medford, MA, USA

²Wyss Institute for Biologically Inspired Engineering at Harvard University, Cambridge, MA, USA

³Lead contact

*Correspondence:
michael.levin@tufts.edu

<https://doi.org/10.1016/j.isci.2021.102131>



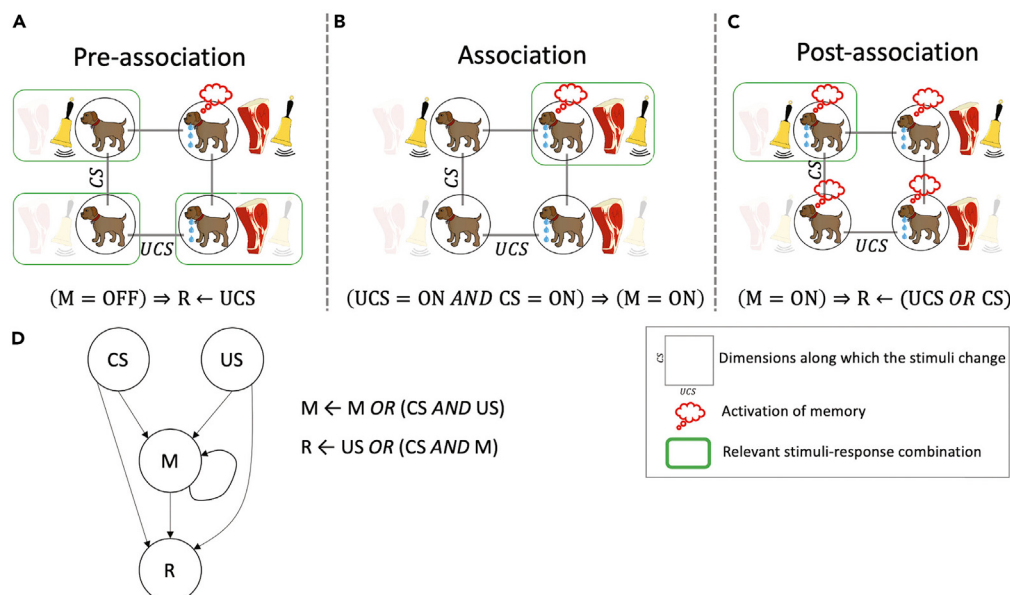


Figure 1. Extending associative learning paradigm to GRNs

The sequence of behavioral changes is driven by particular combinations of stimuli in every phase of associative memory. The stimuli-response mapping is shown for each phase, and the relevant ones are marked with a green box. For example, during the pre-association phase (A), the relevant combinations are where either the individual stimuli or no stimuli are presented. (B) During the association phase, both stimuli are presented at the same time. The most important observation to be made here is the distinction between the stimuli-response mappings of the pre-association and the post-association phases (C). In particular, the salivation response to CS during post-association is altered compared with that in the pre-association phase. This is accomplished by the activation of memory during the association phase. In other words, the dog with a memory of the association between UCS and CS responds to the latter stimulus differently. This altered behavior is a result of memory, as shown by the equation at the bottom of (C). The underlying Boolean network model (D) shows the rules of behavior of the memory (M) and the response (R) nodes. The phenomenon of associative memory can also be understood in symbolic terms as follows. During the pre-association phase M is not activated as per the relevant stimuli-response combinations. Thus, if we set $M = \text{OFF}$ in the rule for R, we get a rule that says that R can be triggered by UCS only ($R \leftarrow \text{UCS}$). During the association phase, the joint presentation of the stimuli activates M. Finally, during the post-association phase, if we set $M = \text{ON}$ in the rule for R, we get a rule that says R can be triggered by either UCS or CS in a symmetrical way ($R \leftarrow \text{UCS OR CS}$). In other words, association casts UCS and CS as equivalent from the point of view of R.

function by modulating the temporal sequence of inputs? This is a different approach from existing conceptions of memory as changes at the epigenetic and protein levels (Corre et al., 2014; Nashun et al., 2015; Quintin et al., 2014; Zediak et al., 2011).

Several prior studies have tested specific memory phenomena in GRN models (Kandel et al., 2014; Levine et al., 2013; Macia et al., 2017; Ryan et al., 2015; Science, 2003; Sible, 2003; Urios et al., 2016; Watson et al., 2010, 2011; Xiong and Ferrell, 2003). However, there has been no systematization of the kinds of memories that such networks could possibly exhibit. We sought to rigorously define several types of memory (loosely analogous to those found in the behavioral science of neural networks), provide an algorithm with which any future network model can be evaluated for interesting memory dynamics (to make predictions for experiment), and compare existing models of important biological networks with those of random networks.

One especially intriguing possibility concerns associative learning (Kohonen, 2012; Palm, 1980). The textbook experiment by Pavlov illustrates associative learning in a specific form known as “classical conditioning” (Lee and Young, 2013; Rescorla, 1967) (Figures 1A–1C). Here, initially, the dog naturally salivates when it smells food, termed the *unconditioned stimulus* (UCS), and does not salivate when it hears a bell ring (Figure 1A), making the bell the *neutral stimulus* (NS). The smell of food and the sound of a bell are unrelated stimuli, and only one, the UCS, induces the dog’s salivation (the *response* R). In this experiment, the dog is exposed to the UCS and NS at the same time repeatedly (Figure 1B). Gradually, the dog learns to associate the NS with the UCS, to the point where it responds to the bell alone as if food is present, functionally

transforming the NS to a *conditioned stimulus* (CS), which can now produce the response R (Figure 1C). Although associative learning is traditionally studied as a neural phenomenon, many different types of dynamical systems can instantiate it (Baluška and Levin, 2016; Fernando et al., 2009; Manicka and Levin, 2019a, 2019b; McGregor et al., 2012) (Figure 1D). Indeed, the original experiments of Pavlov showed associative and other kinds of learning within his dogs' organ systems (Gant, 1974, 1981), in addition to the well-known learning of the animal via its brain.

In biomedical contexts, some drugs targeting specific network nodes are highly effective in laboratory studies but too toxic to use long-term in patients (Frey et al., 2019). If associative memory existed in GRNs, predictive algorithms could be developed to reveal which stimuli can be used to trigger desired responses via a paired "training" paradigm. In this case, the network would associate the effects (R) of a powerful but toxic drug (UCS) with a harmless one (NS, which would become the CS). It might then be possible to treat the patient with the neutral drug (NS) to obtain the desired therapeutic response of the UCS without the side effects (Figure 1D). This is just one example of a number of strategies that can be developed for rational control of GRN function, once the memory properties of GRNs of interest were characterized.

To achieve this, we rigorously systematized the notion of memory in dynamical models of GRNs and similar types of networks and developed algorithms to analyze the plasticity of response to specific node activations over time. Here, we focus on a well-known class of dynamical models known as Boolean networks (BN) that was pioneered by Stuart Kauffman (Kauffman, 1969) and Rene Thomas (Thomas, 1973) as simple coarse-grained models of GRNs. The nodes (variables) in a BN are binary: a state of 0 (OFF) represents repression, whereas 1 (ON) represents activation. Gene states are updated over time due to interactions with other genes and their transcripts, as described by the Boolean functions associated with each node. The Boolean operators defining the relations among the genes are AND, OR, NOT, and XOR (see [Transparent methods](#) for more details). Boolean models have proved to be useful in gaining dynamical insight into numerous phenomena, such as criticality (Kauffman and Strohman, 1994), cell signaling (Saez-Rodriguez et al., 2009), pattern formation and control (Marques-Pita and Rocha, 2013), cancer reprogramming (Zanudo and Albert, 2015), drug resistance (Eduati et al., 2017), and even memory in plants (Demongeot et al., 2019); the Cell Collective model database (Helikar et al., 2012) that we utilize in this work contains many more such published examples. For comprehensive reviews of BNs, including aspects of how they are inferred, analyzed, and used to make predictions, see Albert et al. (2008), Albert and Thakar (2014), Albert (2004), and Wang et al. (2012).

We hypothesized that GRNs in general may be capable of diverse new kinds of memory, in that their response to future node activation events would change to implement the desired network behavior, and that an algorithm could discover the necessary sequence of stimuli to make this occur predictably. Such long-term change in behavior due to experience (memory) could occur via changes at the level of the dynamical system state space, not requiring changes in inductive/repressive relationships between genes (rewiring the connectivity). We specifically hypothesized that such historicity would be an inherent property of networks but would be significantly enriched in real biological GRNs. It is important to note that the memory being tested here takes place within the lifetime of a single, constant GRN, rather than during a process of evolutionary selection or population learning.

If found, long-term changes in GRNs' dynamical system states would be analogous to intrinsic plasticity in neuroscience, which functions alongside synaptic plasticity (rewiring that changes the connection weights between nodes). There is increasing biological evidence that learning and memory happen at the level of single neurons and that memory could be stored in their dynamic activities as intrinsic plasticity due to the dynamics of bioelectric circuits (Banerjee, 2015; Daoudal and Debanne, 2003; Debanne et al., 2003; Gal-lahe et al., 2010; Geukes Foppen et al., 2002; Izquierdo et al., 2008; Law and Levin, 2015; Snipas et al., 2016). The theoretical foundations of such plasticity-free learning have been explored (Stockwell et al., 2015; Yamauchi and Beer, 1994). Thus, the existence of plasticity-free memory in GRNs would have major implications along several lines. First, it would suggest novel developmental programs where dynamic gene expression could result from GRNs whose functional behavior was shaped by prior biochemical interactions and not genetically hardwired. Second, it would suggest a new approach to biomedical interventions complementing gene therapy: drug strategies with temporally controlled delivery regimes could be designed to train GRNs to produce specific outcomes, shape their responses to drug and other interventions in the future, disrupt cancer cells' adaptation to therapeutics, or prevent disease states from arising in

Legend					Before Training			UCS should trigger R	NS should not trigger R
	ON	Off	Repeated	Relaxed	Time	t ₀	t _j	t _{j+1}	
Unconditioned stimulus (UCS)									
Neutral stimulus (NS)									
Response (R)									

Memory Evaluation												
Memory Types	Training			Testing								
	t ₁t _j	t _{j+1}	t _{j+2}t _k	t _{k+1}	t _{k+2}	t _{k+3}	t _{k+4}t _j	.t _{j+1}				
UCS Based							Once activated, Response stays even though stimulus is gone.					
Pairing							UCS requires pairing with another, NS, in order to make Response stable after UCS stops.					
Transfer								After repeated UCS, another, NS, is able to induce R				
Associative								After pairing UCS and NS, the NS alone is able to turn on R (becomes a CS). Once associates the NS can turn on R repeatedly.				
Consolidation												

Figure 2. Definition of different memory types

UCS and NS input stimuli are schematized as switches, whereas response R is schematized as ON/OFF electric bulb. To represent the ON, OFF, Repeated, and Relaxed states of UCS and NS, blue and green switches with different positions are used, respectively. We define the pre-requisites for memory testing in the block headed as Before training. It requires that initially (at time t₀) UCS, NS, and R should be OFF, and such that UCS triggers R and NS does not trigger R. The memory evaluation table describes each memory type as a row. The five broad memory types are described here as UCS Based, Pairing, Transfer, Associative, and Consolidation memory. For each memory evaluation, there are training and testing phases, showing the overall dynamic and what is learned (the stable change in system behavior) over time.

specific circumstances. Moreover, an understanding of GRNs' long-term modification by prior physiological experiences could help explain the wide divergence of drug efficacy and side effects across patients and even across clonal model systems (Durant et al., 2017).

The presence of a kind of learning in GRNs has been suggested in specific cases (Deritei et al., 2019; Fernando et al., 2009; Herrera-Delgado et al., 2018; Sherrington and Wong, 1989, 1990; Stockwell et al., 2015; Tagkopoulos et al., 2008; Zañudo et al., 2017), but there has been no systematic study of memory across diverse GRNs or analysis of possible different kinds of memories that may exist and the relationships between them. Moreover, plasticity in the form of changes to the weights of connections, or mechanisms, is generally thought to be required for memory in GRNs. It is also unknown whether memory is a property of all networks (e.g., random ones) or whether biological GRNs exhibit unique memory types or increased propensity for memory. Here, we comparatively analyze the definitions of memory in the context of animal behavior, mapping them onto possible GRN dynamics, providing a taxonomy of learning types appropriate for GRNs and other networks like protein pathways, all without any changes to weights or mechanisms. We rigorously define the kinds of memory that could be present in GRNs (Figures 2 and S1) and then produce an algorithm (Figure S2) to systematically test any given GRN for the presence of different types of memory with different choices of network nodes as stimuli targets.

Analyzing a database of known GRNs ([Table S1](#)) from a wide range of biological taxa, we show that several kinds of memory can be found, including associative memory. We develop configuration models (randomized versions of each biological GRN) to demonstrate that the amount of memory found in a GRN is not governed solely by the node number and edge density, and that real biological GRNs are distinct in their types and degrees of memory compared with similar random networks. Comparing GRN data with analysis of configuration models revealed that the biological networks have disproportionately more memory (suggesting that biological evolution may have favored networks with memory properties). We also identified statistical relationships between the likelihood of a given network exhibiting a particular kind of memory and two factors: what other memory types it may have and what kind of cell or organism the GRN is from. Taken together, our results provide a novel way to understand and control GRN behavior, establishing a software framework for discovery of memory, and thus for actionable intervention strategies for biomedical, developmental, and synthetic biology settings.

RESULTS

Transcriptional networks can exhibit multiple kinds of memory

A GRN is a model of transcriptional control consisting of genes and their mutual regulations ([Blais and Dynlach, 2005](#); [De Jong, 2002](#)). Each gene has a basal expression level that applies when the gene is neither regulated by any external stimuli nor influenced by other genes (through their encoded proteins). Basal expression levels change when a gene is activated via regulation, which then in turn may modulate others ([Macneil and Walhout, 2011](#); [Samal and Jain, 2008](#)). We designate the activation of some nodes as “inputs” (corresponding to specific sensory experiences that an animal may receive from its environment) and the activation of another node R as a “response” (corresponding to a discrete behavior that can be produced under specific circumstances). We define “training” in this context as the stimulation of some of the network nodes in a specific pattern to induce long-lasting changes in how the network responds to node activation events in the future.

We formally define “memory” ([Figure 2](#)) in this context as a phenomenon describing the relationship between two sets of genes, namely, “stimulus” and “response” that satisfies the following conditions: (1) the stimulus activates the response and (2) the response retains its activation state even after deactivation of the stimulus (the existence of history). The fundamental signature of memory is its temporality—a long-lasting and stimulus-specific change induced by a transient experience ([Bacchus et al., 2013](#); [Chechile, 2018](#); [Durso and Nickerson, 1999](#); [Weitz and Simmel, 2012](#)). We consider individual nodes of a Boolean GRN as the potential targets of external stimuli and able to produce a response (output or effector nodes). For example, a specific transcript can be upregulated by some exogenous factor triggering its expression, and the appearance of a given gene product (e.g., secretion of an important hormone or growth factor) can be considered the circuit’s response. For applications, we are especially interested in nodes that can be readily stimulated with small-molecule drugs, and for response, we are interested in nodes that control key drivers of health and disease (e.g., the levels of calcium, pH, immune activation, cell differentiation, etc.). The challenge then, for any given network and response of interest, is to computationally identify the correct nodes that may serve as inputs, as well as a temporal stimulation regime for those stimulus node(s) that will result in desired changes in response activity over time.

Specifically, we consider two types of stimulus nodes, namely, unconditional stimulus (UCS) and neutral stimulus (NS), and a single response node (R). The first type of stimulus, UCS, is capable of triggering R, and the second type, NS, is initially neutral to R but may be conditioned such that it becomes a driver to activate R. In classical conditioning of a GRN, we pair the NS with the UCS and apply both repeatedly so that the system can learn the association between the two stimuli and functionally link the NS with the state of R. Later, we test to see if R is now driven by the NS alone (if true, NS can now be called a conditioned stimulus [CS]). The taxonomy of possible memory types in such systems, and their relationships, are schematized in [Figure 2](#), including UCS-based memory (UM, long-term response induction by a specific stimulus), pairing memory (PM, one-shot stabilization of response to compound cues), transfer memory (TM, resembling discrimination training that results in a more generalized response), associative memory (AM, including two of its sub-categories: long recall associative memory [LRAM] and short recall associative memory [SRAM]), and consolidation memory (CM).

We tested (using the algorithm shown in [Figure S2](#)) many models of a diverse range of biological systems (networks with fewer than 25 nodes) obtained from the publicly available dataset *Cell Collective* ([Helikar](#)

et al., 2012) for each of the kinds of memory using the criteria in Figures S1 and 2. A key aspect of our algorithm is that for any given GRN to be analyzed, the algorithm tests all the combinations of different nodes for their ability to serve as NS, CS, UCS, and R in the various assays. Thus, for any given network (or set of networks), one can compute the prevalence of memories—what percentage of all possible combinations of choices of nodes as NS, UCS, and R give rise to different kinds of memories. Figure 3 describes the structure function of a Boolean GRN, the network simulation for UCS-based memory evaluation, and overall memory estimation of a GRN with an example of a small GRN named Cortical Area Development GRN.

The raw data in each of the training and testing phases for AM are shown in Figure 4 (representative data for the other memory types are shown in Figures S3–S6), using the Mammalian Cell Cycle 2006 network and suitable choices of nodes for NS, CS, UCS, and R as an example (Figure 4A). The Boolean equations corresponding to this GRN and each of other GRNs tested in this article (as given in the GRN repository) can be found in Data S1. The pre-requisite conditions (Figure 4B), for an appropriate choice of nodes to serve as UCS, NS, and R (see Figure 3B) out of all possible choices of nodes for these roles, are that UCS alone should be sufficient to trigger R and that NS alone does not trigger R before training and memory evaluation. The training phase (Figure 4C) shows pairing of UCS and NS activations. After successful training, the NS alone becomes sufficient to trigger R (Figure 4D); it is seen that the NS has in fact become a conditioned stimulus because when it stops, the response stops, and when it is presented again, the response begins again (Figure 4E). This fulfills the basic criteria of Pavlovian conditioning (Figure 1) and shows that the functional roles of the input nodes with respect to GRN behavior have been stably altered by experience of stimuli, the pairing of two node activations during training (Figure 4C). It should be noted that in identifying specific nodes as effective CS, UCS, and R nodes for a given instance of memory, it is not the case that the memory somehow resides in those three nodes: memories are a function of the entire network, distributed therein and revealed as experience-dependent changes of network-wide activity by stimulation and readout at specific nodes chosen as inputs and outputs.

We sought to discover minimal networks showing each kind of memory, to serve as prototypical examples clarifying the logic of each type of memory, and to guide the design of novel GRNs for synthetic biology applications that could exploit transcriptional dynamics for memory functions. At minimum a network needs two nodes (UCS and R) to form UM and three nodes (UCS, R, and NS) to form any other type of memories. To test the topographies and motifs associated with each type of memory, we created 10,000 random Boolean networks (RBNS) for each case and evaluated each memory using our toolkit (see *Transparent methods*). The smallest networks discovered to be sufficient for each type of memory are shown in Figure 5. We conclude that even fairly simple networks, readily accessible to synthetic biology construction, can give rise to memory functionality.

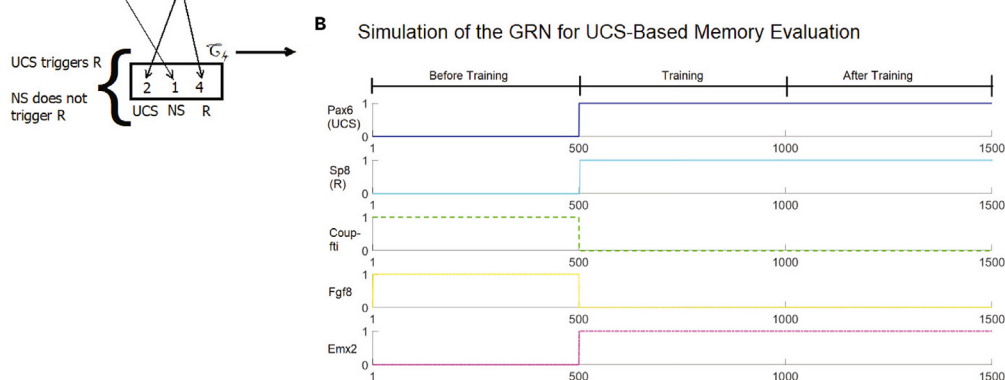
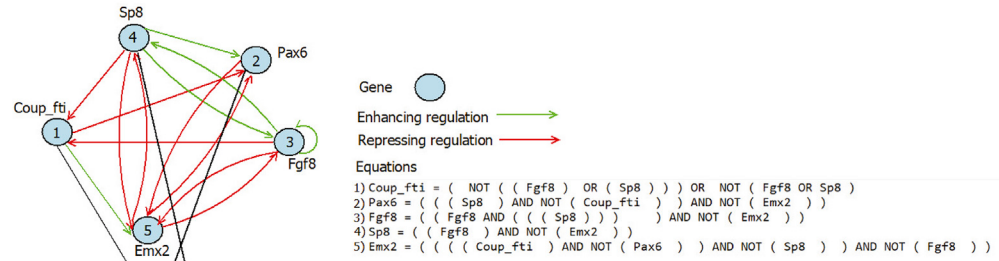
Biological GRNs possess various memory types: an analysis across taxa

We tested 35 biological GRNs (those <25 nodes in size, from Cell Collective (Helikar et al., 2012); Data S1 provides Boolean equations for each GRN obtained from the same website) for each kind of memory (Figure 6A). These included GRNs at different strata of the tree of life (prokaryotes and eukaryotes), cancer, diverse metabolic processes in adult and embryonic stages of mammals, cellular signaling pathways in invertebrate and plants, etc. For each network, the prevalence of each type of memory was analyzed by assessing the number of different combinations of nodes that can serve as UCS-R-NS.

Three of 35 (8.57%) GRNs exhibited no feasible stimuli-response (UCS-R-NS) combinations exhibiting memory. For those GRNs with memories (32 out of 35), UM was the most prevalent type of memory, followed by TM. AM and PM memory types were somewhat rarer (only 5 of 35 GRNs). AM appeared in "Aurora Kinase A in Neuroblastoma," "B cell differentiation," "CD4+ T Cell Differentiation and Plasticity," "Cell Cycle Transcription by Coupled CDK and Network Oscillators," "Mammalian Cell Cycle 2006," and "Neurotransmitter Signaling Pathway" GRNs, among which the first and the third GRNs (highlighting one combination of stimuli-response for each) are shown in Figures 6B and 6C respectively. In each of the first three and the last GRNs, AM and PM occurred together. For each GRN, the percentage of combinations where a certain memory appeared out of all feasible combinations is listed in Table S2.

We then asked whether there is any grouping of the different GRNs that reveals a pattern—is predictive for the presence of memory capacity. Although it is difficult to define categories that objectively and unambiguously sort the available GRNs into sharp classes, we considered two simple, rough categorizations of

A Cortical Area Development GRN: A real GRN with associated equations



C Calculation of Overall Memory in the GRN

All possible Stimuli-Response combinations	Memory evaluation schemes					
	UM	PM	TM	AM	CM	NM
G_1	1	0	1	0	0	0
G_2	1	0	0	0	0	0
G_3	1	0	0	0	0	0
G_4	1	0	1	0	0	0
⋮	⋮	⋮	⋮	⋮	⋮	⋮
G_{19}	0	0	0	0	0	1
Memory in GRN	$\frac{\sum \text{UM}}{19} \times 100$	$\frac{\sum \text{PM}}{19} \times 100$	$\frac{\sum \text{TM}}{19} \times 100$	$\frac{\sum \text{AM}}{19} \times 100$	$\frac{\sum \text{CM}}{19} \times 100$	$\frac{\sum \text{NM}}{19} \times 100$

1 = Memory found
0 = no memory found

Figure 3. Description, simulation, and overall memory evaluation of Cortical Area Development GRN

This figure provides the description of topology, simulation outcome, and overall memory evaluation procedure of a Boolean GRN with an example of a small 5-node GRN, named Cortical Area Development GRN.

(A) Here we provide the topology of the Cortical Area Development GRN and the set of Boolean equations required to simulate it. In the topology, a gene is represented with a blue circle and enhancing and repressive regulations are represented with green and red arrowheads, respectively.

(B) Here we show the criteria of choosing a feasible stimuli-response combination and the simulation of the GRN activating chosen stimuli in the training phase of memory evaluation. We observe that both the stimulus (Pax6 gene treated as UCS) and response (Sp8 gene treated as R) are in low state before training. We make the stimulus high (flip) and clamp it in high state during training. We unclamp UCS at the end of training and detect R, retaining the memory of its state during training phase. Here, UCS also keeps itself in high state through the post-training period by some internal mechanism. It should be noted that as we do not require NS in UCS-based memory evaluation presented here, we treat Coup-fti of the stimuli-response combination as a normal gene.

(C) Here we show the memory evaluation procedure of the whole GRN. Out of all possible node combinations treated as UCS, NS, and R we obtain 19 feasible combinations where UCS triggers R and NS does not trigger R. For each such combination, we separately perform each type of memory evaluation and list the results in the table. If a test passes, we put a 1, 0 otherwise. We calculate the percentage of each type of memory in the GRN, treating total memory as 100% for the network.

GRNs: one based on whether they belong to vertebrates or invertebrates and the other based on whether they belong to generic or unicellular cell activities versus specific cell types in metazoan bodies. We found that both the vertebrate/invertebrate and the cell specificity distinctions are excellent predictors (with an

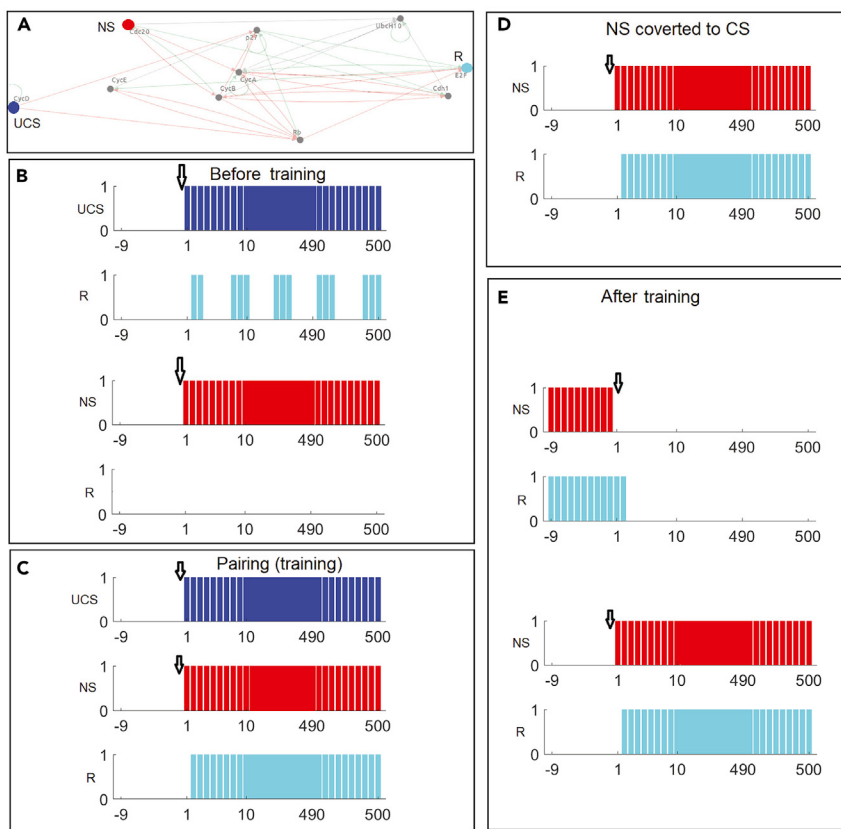


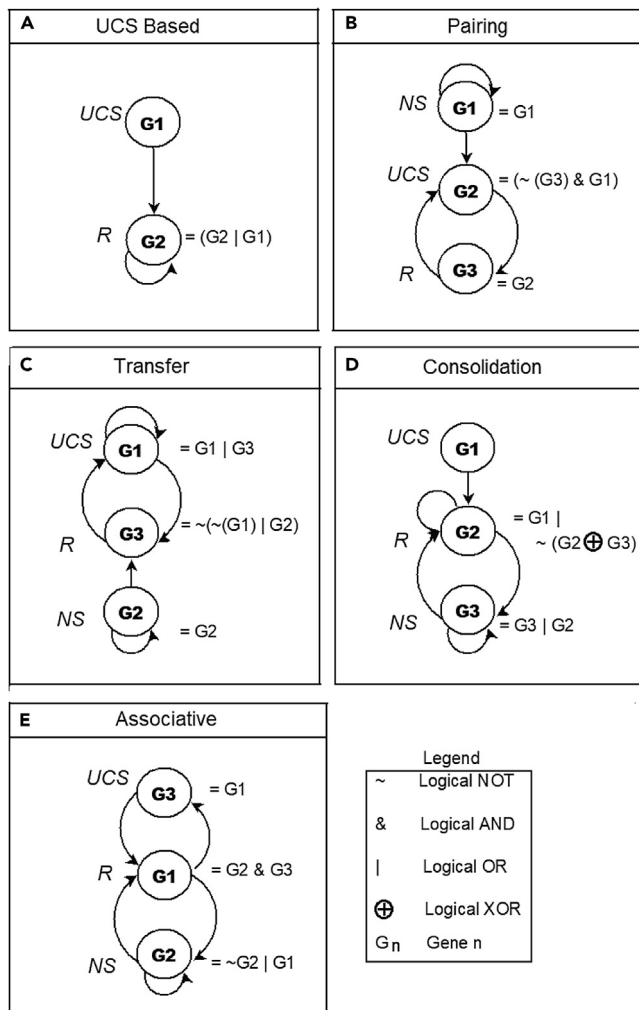
Figure 4. Time series data of a GRN's evaluation for associative memory

This trace describes the run time state changes in evaluating associative memory of a mammalian cell cycle network.
 (A) In the mammalian cell cycle network 2006, the genes used as UCS, NS/CS, and R are highlighted with blue, red, and cyan respectively. With these respective colors the states of UCS, NS/CS, and R in different plots are defined. A downward arrow in each plot shows the start of the activation of the corresponding stimuli. In each panel, we show the 10 past states of a stimulus to depict its state change upon the activation at time 0.
 (B) The resultant states of R, observed from activation of UCS and NS, respectively, before training: R gets activated with onset of UCS but NS cannot trigger R.
 (C) Pairing (training) experiment shows the successful activation of R.
 (D) After training, activation of the previously neutral stimulus causes R to be activated, confirming that the experience of paired stimuli has converted the NS node to a CS.
 (E) As further confirmation of stable causality established between CS and R by training, we first deactivate CS, to see if R gets deactivated, and then reactivate the CS to ensure that it can activate R again.

accuracy of 74% and 86%, respectively) of the existence of memory, as evidenced by their performance as classifiers of prevalence of memory (Figure 7). Thus, we conclude that a diverse set of biological GRN structures exhibit various types of memory, which are especially highly represented within differentiated cells of vertebrate organisms.

Memory types and their relative prevalence among possible GRNs

Do larger networks in general have more memory capacity than smaller ones? To better understand the properties that underlie memory in networks, we generated RBNs to test different aspects of network structure. To determine how memory in RBNs changes with increasing network size, we created RBNs ranging in size from 5 to 25 nodes, with 100 RBNs generated for each size range (see Table S7). We evaluated the pool of RBNs of each size separately to observe the change of average memory distribution with the increase in size. We found that memory is less common in smaller RBNs (under 15 nodes in size, Figures 8A and 8D) and restricted to UM- and TM-type memory. Other types of memory start appearing in RBNs with 15 or more nodes. Although UM dominates, all memory types were observed (Figures 8B–8D), with increasing amounts of the non-UM memory types at network sizes of 20 and 25 (Figures 8C and 8D). Interestingly,

**Figure 5. Minimal RBNs have distinct memory types**

(A–E) Minimal BNs of the memory types (A) UM, (B) PM, (C) TM, (D) CM, and (E) AM. Each node of a network shows the Boolean equation matching the description of the relationship between the nodes. We present the symbols used in the equations in the legend.

in 15 and 20 node networks, LRAM is more common than SRAM, but in 25 node RBNs, SRAM dominates (Figures 8B–8D). We then asked whether the same relationship between network size and likelihood of memory holds in biological networks. We grouped the 35 biological GRNs into 5 categories with network size 5–9 (2 GRNs), 10–14 (6 GRNs), 15–19 (14 GRNs), 20–24 (10 GRNs), and 25–25 (3 GRNs). We evaluated memory and presented average memory distribution in the same manner as RBNs. We observed that GRNs have large amount of memories across networks, but, like RBNs, the percentage of networks with memory increases with network size. Availability and proportion of different types of memories in GRNs (Figures 8E–8H) are not entirely size dependent, although this relationship will become better quantified for biological networks when larger numbers of GRNs become available at different size ranges.

We next asked whether the likelihood of finding memories in networks of different sizes was similar in biological GRNs as in randomly constructed networks: is there anything special about how memories are distributed in biological networks of various sizes? For each type of memory in a GRN, we observed how its prevalence fits into the probability distribution of the corresponding values of 100 RBNs of similar size. To determine whether the size/memory relationship in biological GRNs is in any way unique (distinct from that observed in random networks), we calculated p values (Table S3) and performed an outlier test (Table S4) comparing the distributions in Figure 8. The null hypothesis is that the distributions of GRN

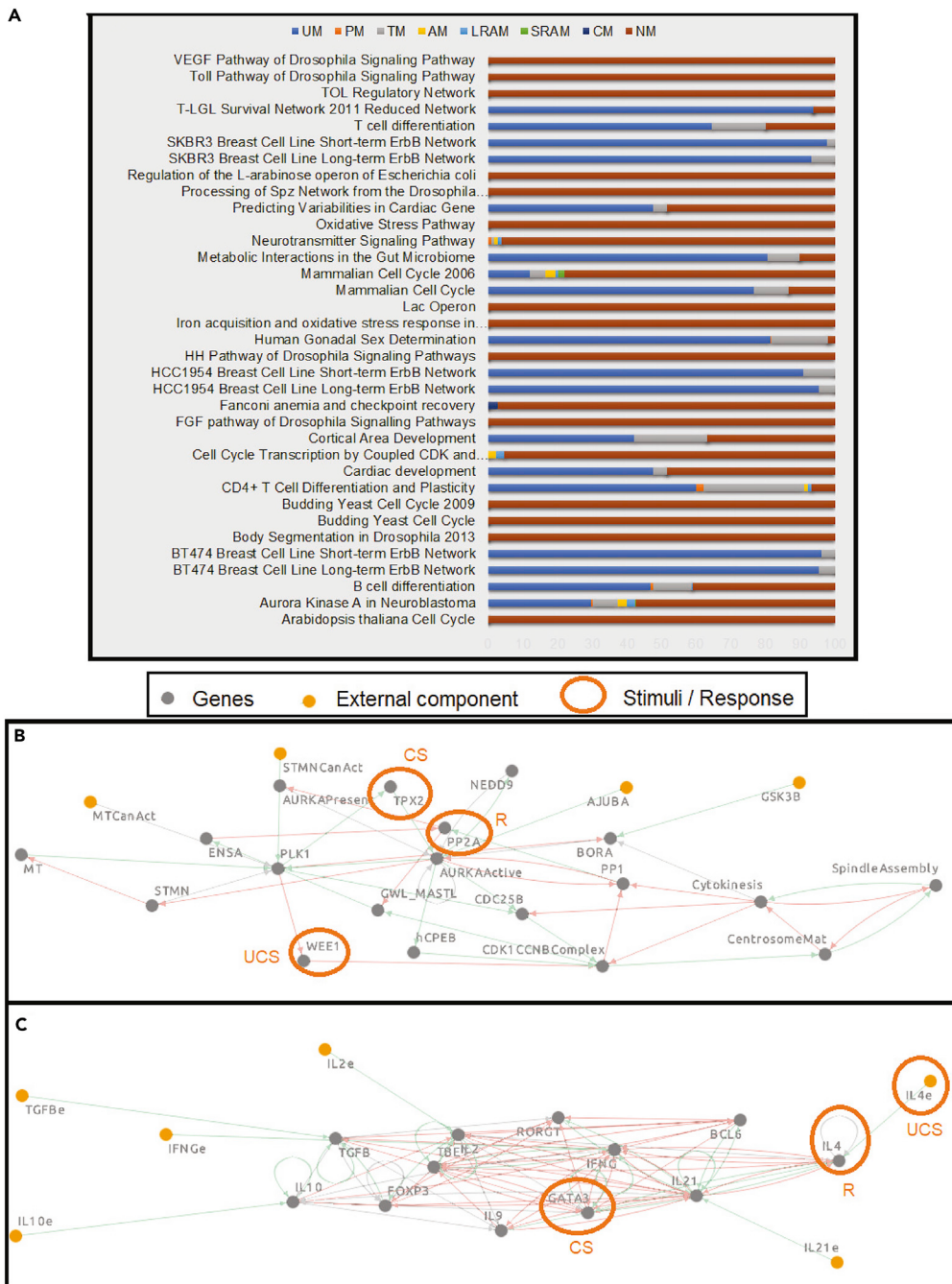


Figure 6. Associative memory in biological GRNs

(A and B) (A) Types of memory found in each of the 35 GRNs taken from the Cell Collective database. Associative memory was found in two of the GRNs: Aurora Kinase A in Neuroblastoma (B) and CD4+ T cell Differentiation and Plasticity (B). For each network, we present an example of the stimuli-response combination where AM is obtained. (A) Cell Collective network where 3 genes, WEE1, PP2A, and TPX2, act as UCS, R, and CS respectively. Activating TPX2 together with WEE1 enables TPX2 to activate PP2A, whereas previously only WEE1 did so.

(C) Cell Collective network where IL4e, IL4, and GATA3, respectively, act as UCS, R, and CS. Activating GATA3 together with IL4e enables GATA3 to activate IL4, whereas previously only gene IL4e did so.

memories across size categories are not different from the memories of similar-sized RBNs. If the outlier test is passed for a given memory type, this would indicate rejection of null hypothesis: GRN memory distributions are different from those found in similar RBNs. In each analysis, we obtained a matrix (35 GRNs

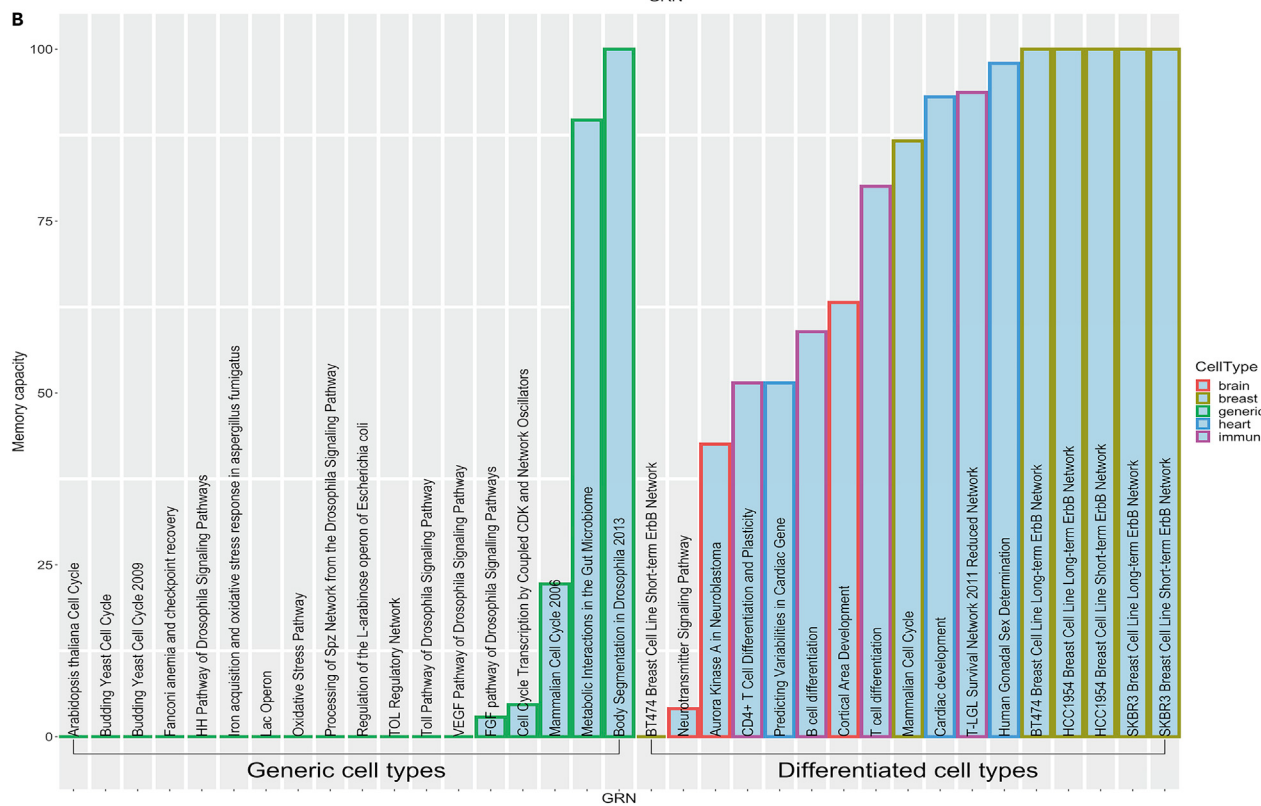
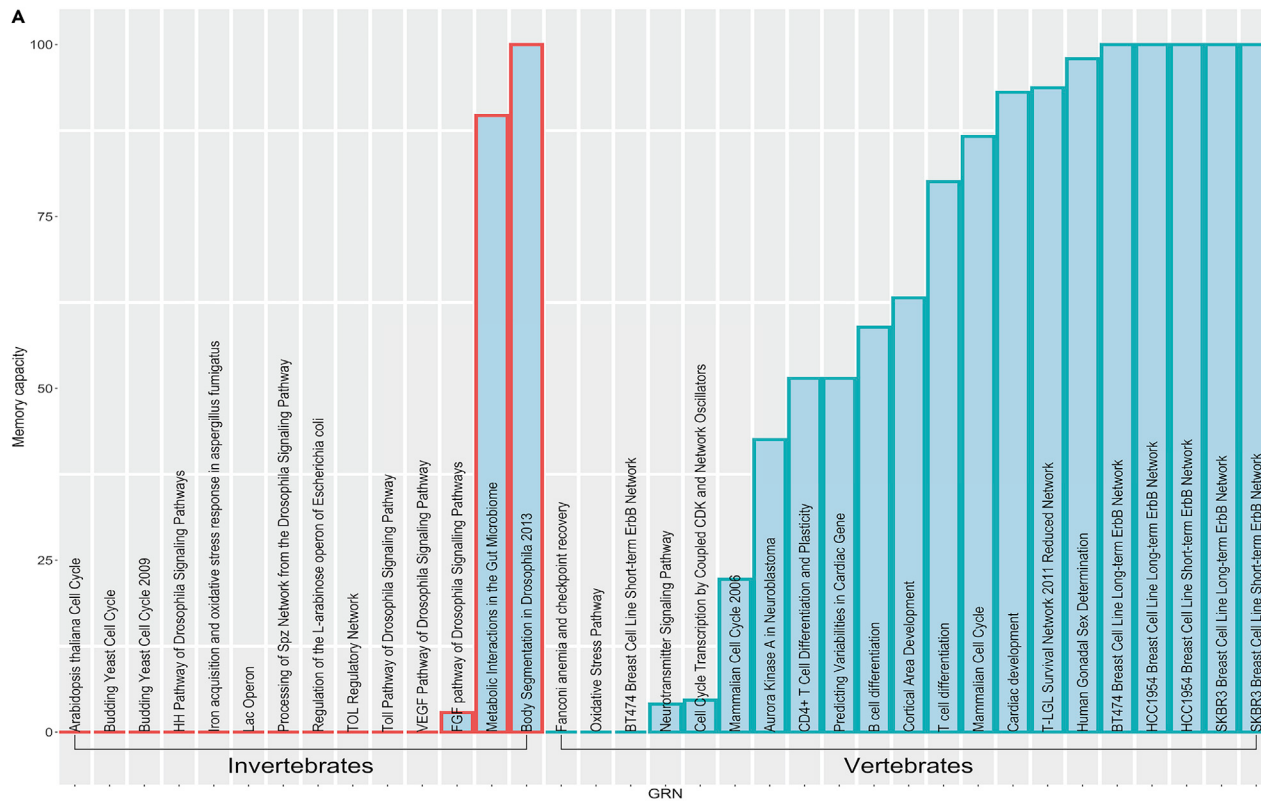


Figure 7. Distribution of different memory types across diverse biological systems

(A and B) The memory capacity of GRNs can be systematically classified according to their features. (A) A classification of GRNs based on whether they correspond to vertebrate or invertebrate species. This panel shows that vertebrate GRNs tend to contain more memory than the invertebrates, as quantified by the classification performance metrics: Accuracy = 0.74, Sensitivity = 0.88, Specificity = 0.63, Positive predictive value = 0.67, Negative predictive value = 0.86, and AUC = 0.75. Red borders indicate data from invertebrate GRNs, whereas green borders indicate data from vertebrate GRNs. (B) A classification of GRNs based on whether they derived from a unicellular or generic process or from a specific somatic cell type. This panel shows that the GRNs corresponding to the non-generic cell types tend to contain more memory than the generic ones, as quantified by the classification performance metrics: Accuracy = 0.86, Sensitivity = 0.88, Specificity = 0.84, Positive predictive value = 0.82, Negative predictive value = 0.89, and AUC = 0.86. Classification was performed as follows. First, the memory capacity of each GRN was computed as the proportion of memory within the total that included the "no-memory" type. Then, if the memory capacity of a GRN exceeded 50% it was categorized under the "memory" class or in the "no memory" class otherwise. The standard binary classification metrics reported above were computed based on the associated confusion matrix containing the number of True-Positives (TP), False-Positives (FP), True-Negatives (TN), and False-Negatives (FN) where the "memory" class is the "positive" class and the "no-memory" class is the "negative" class. As per standard definitions, Accuracy is the proportion of TP and TN among the total number of instances, Sensitivity is the proportion of TP among the actual positive instances, Specificity is the proportion of TN among the actual negative instances, Positive predictive value is the proportion of TP among the predicted positive instances, Negative predictive value is the proportion of TN among the predicted negative instances, and AUC is the area under the receiver operating characteristic curve, which can be interpreted as the probability that the classifier will rank a randomly chosen positive instance higher than a randomly chosen negative instance.

each having 8 types of memory, including no memory). In the first case, each element of the matrix is a p value [0, 1]. We considered significance when $p < 0.05$. In the second case, the value is binary (1 if the value is an outlier in the distribution of similar-sized 100 RBNs; 0 otherwise). Using either test, the percentage of significant deviations from random distributions was relatively higher for UM and TM when compared with other memory types.

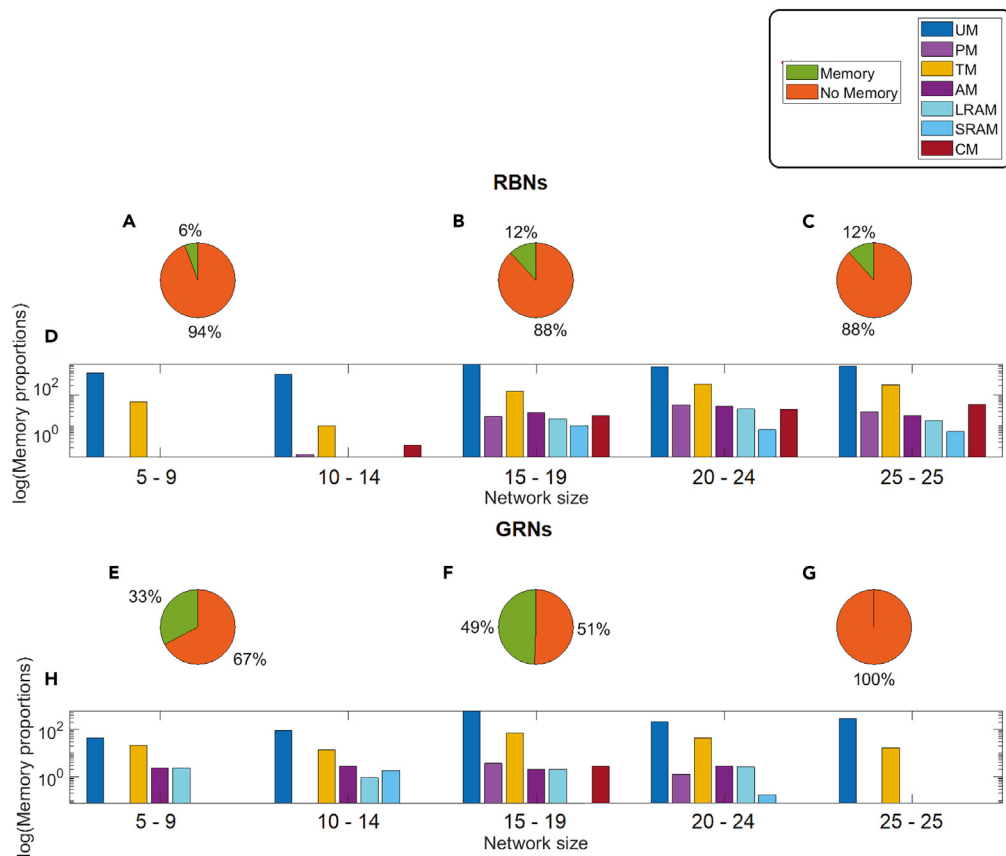
To confirm the differences between the class of biological GRNs and random counterparts, we also conducted Fisher's exact test to determine whether GRNs and RBNs are statistically different. For 3 categories of GRNs we tested network sizes of 5–9 (small), 15–19 (intermediate), and 25–25 (large). Using contingency tables of memory versus no memory in GRN and similar-sized RBNs, for all the 3 cases, the null hypothesis that occurrences of memory in GRNs and RBNs are not different was rejected with p values 2.0E-05, 7.4E-323, and 4.4E-323, respectively. Taken together, our statistical analyses show that biological GRNs have unique distributions of memory types with respect to network size.

The memory profile of biological GRNs is unique

Do real biological networks' topologies offer more opportunities for memory dynamics than would be expected by chance in arbitrary networks of similar size and type? We generated 3500 "configuration models"—100 randomized versions for each biological GRN—and analyzed them for the presence and prevalence of each memory type. We then used statistical tests to compare these aggregate statistics to the memory profiles of the 35 actual biological networks, to determine whether GRNs of biological origin are in any way special with respect to memory capacity over what is provided by the generic properties of BNs. We note that comparisons across different types of GRNs are limited by the set of available specific GRNs; thus, future analyses of a broader set of GRNs emerging from this field are likely to refine and expand our results.

Given a certain type of memory in a GRN, we checked to see how the value fits into the probability distribution of the corresponding values of its ensemble. We calculated p values (Table S5) and conducted an outlier test (Table S6). In each type of analysis, we obtained a matrix (35 GRNs each having 8 types of memory, including no memory). In the p value test each matrix element was a p value [0, 1]. We considered significance when $p < 0.05$. In the outlier test, the value was binary (1: if the value is an outlier in its random ensemble; 0: otherwise). In either test, the percentage of success was relatively high for UM and TM compared with others.

Furthermore, we examined how each type of memory in a GRN fits into its random ensemble, visualizing the distribution of memories via violin plots (Hoffmann, 2015). We found (Figure 9A) that the incidence of memory-containing biological GRNs is generally unique with respect to possible GRNs, lying outside the [5 95] percentile bars. Thus, we found that the data are not compatible with memory profiles in biological networks occurring solely as a consequence of the generic mathematical dynamics of BNs (Kauffman, 1993). The fact that distribution of memories across real biological networks differs from that of randomized networks suggests that biological evolution has given rise to GRNs with specific memory properties. Our data do not distinguish between direct selection for memory in GRNs and indirect selection in which

**Figure 8. Distribution of memory in different sizes of RBNs**

(A–C) Pie charts show the memory distributions in RBNs with 5, 15, and 25 nodes (100 RBNs for each case).

(D) Comparative distribution of different memories in various sizes (5, 10, 15, 20, and 25) of RBNs.

(E–G) Pie charts show the memory versus no memory distribution in GRNs.

(H) Comparative distribution of different memory types across biological GRNs of increasing size.

memory is favored because it enables some other feature with selective advantage (e.g., plasticity of physiological response).

Memories in biological GRNs do not occur independently

As different kinds of memories have not before been rigorously defined for GRNs, or examined across the broad range of possible networks, it was not known whether memories tend to occur in the space of GRN topologies independently or whether certain GRN structures simultaneously predispose the network to multiple types of memories (perhaps distributed across different sets of CS/UCS nodes). Thus, we next sought to characterize possible relationships between the incidence of distinct memories in a wide range of possible networks. Having generated a large number of configuration models, we asked whether the presence of one type of memory is statistically related to the likelihood of finding any other memories. We found that conditional entropy (quantifying ordered correlation) between two types of memories in biological GRNs (Figure 8B) is much higher than that of their randomized configuration models (Figure 9C). Correlation between AM (especially LRAM) and any other memory type (not including SRAM and CM) is especially significant. Biological GRNs show tight correlations between UM and TM. Moreover, in biological GRNs, PM predicts the existence of both UM and TM, but the correlation does not hold for the reverse direction, whereas CM implies you will find UM. In the case of configuration models, the sub-categories of AM (LRAM and SRAM) showed correlation to AM. We conclude that the potentials for forming different kinds of memories are not independent, that specific GRN architectures tend to simultaneously support more than one kind of memory, and that the existence of some types of memory can be predicted solely based on the finding of other types.

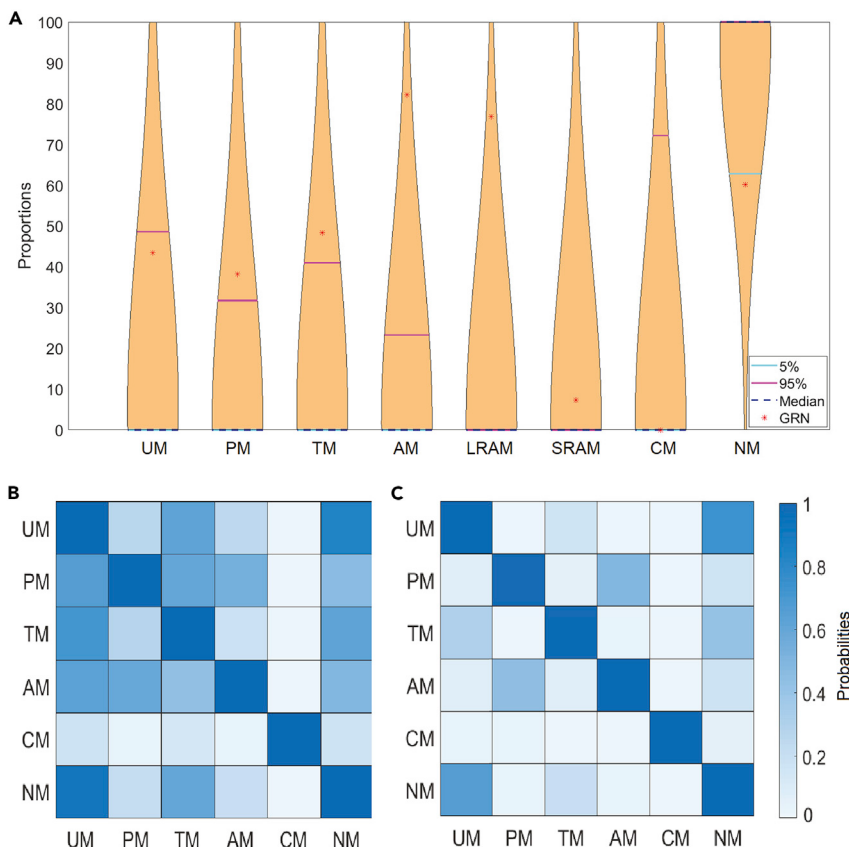


Figure 9. Biological GRNs exhibit unique memory properties

(A) Violin plots of the set of GRNs from the *Cell Collective* database (<https://cellcollective.org/>) are compared (in terms of memories) with their configuration models. We show the median (violet dashed line), 5th percentile (teal line), and 95th percentile (pink line). The actual frequency of memory of the real GRN is represented as a red star. Only the “Aurora Kinase in Neuroblastoma” network from *Cell Collective* is plotted. The violin plots of memories for all the 35 GRNs are given in *Supplemental information (Data S2)*, plots 1–35. We calculated the conditional entropy among the different types of memories of GRNs and configuration models, normalized these conditional entropies, applied Gaussian smoothing, and visualized the results obtained from (B) GRNs and (C) configuration models. Notably, GRNs are different from their randomized counterparts in terms of how much the appearance of one type of memory implies (predicts) the existence of any other type of memory (i.e., biological GRNs have more functional linkage among the different types of memory than is expected by chance).

DISCUSSION

Numerous problems in biomedicine and fundamental life sciences face the inverse problem that affects all complex emergent systems: how do we control system-level behaviors by manipulating individual components? This problem is as salient for bioengineers and clinicians seeking to regulate gene expression cascades as for evolutionary developmental biologists seeking to understand how living systems efficiently regulate themselves (Crommelinck et al., 2006; Karsenti, 2008). An important direction in this field is the discovery of strategies that exploit patterns of input (experiences), rather than hardware rewiring, to achieve desired changes in network behavior or explain the modification of pathway properties faster than occurs during evolution. This strategy requires the development of algorithms to identify specific patterns of stimuli that exert stable, long-term changes in behavior, thus characterizing endogenous memory properties of the system.

We wondered if it were possible to train gene regulatory networks, providing targeted patterns of stimuli to stably change their behavior at the dynamical system level, rather than rewiring network topology at the genetic or chromatin epigenetic levels. This would take advantage of existing computational capabilities of the system and effectively offload much of the computational complexity inherent in trying to manage

GRN function from the bottom up. Such approaches (Pezzulo and Levin, 2016), if the GRN structures were amenable to them, would enable the experimenter, clinician, and indeed the biological system itself to reap the same benefits as training provides for neural systems. Thus, here we performed a systematic and rigorous analysis of memory in Boolean GRNs, an important model of gene regulation that has previously been explored in other aspects (Barberis and Helikar, 2019; Bornholdt and Kauffman, 2019; Demon-geot et al., 2019; Lähdesmäki et al., 2003; Martin et al., 2007; Thomas et al., 2014; Tyson et al., 2019; Wery et al., 2019).

This approach was also motivated by advances in neuroscience that reveal how nervous systems and artificial neural networks learn from experience. Recent studies in the field of basal cognition (memory in aneural and pre-neural organisms [Baluška and Levin, 2016]) have revealed a broad class of systems, from molecular networks (Szabó et al., 2012) to physiological networks in somatic organs (Goel and Mehta, 2013; Turner et al., 2002), that exhibit plasticity and history-based remodeling. Could GRNs likewise exhibit history-dependent behavior that could help explain variability and be exploited to control their function by modulating the temporal sequence of inputs? Based on the remarkable flexibility observed at the anatomical and physiological levels (Blackiston and Levin, 2013; Emmons-Bell et al., 2019; Levin, 2014; Schreier et al., 2017; Soen et al., 2015; Sullivan et al., 2016), and the conceptual similarity between GRNs and neural networks (Sorek et al., 2013; Watson et al., 2010, 2014), we first established a formalization of memory types for GRNs and implemented a suite of computational tests that reveal trainability in a given GRN (Figures 2 and 3). We next created and tested thousands of 2-node and 3-node networks to identify minimal networks exhibiting each type of memory (Figure 4). These motifs can be sought in novel networks as they are discovered, or used as templates for construction of synthetic biology circuits with desired computational properties.

Then we tested different types of BNs from a variety of sources (Figure 5). Our toolkit takes each network as input, generates the feasible UCS-R-NS combinations, evaluates the type of memory(s) in the current combination, counts the number of combinations for each type of memory (including combinations where no memory appeared), and returns these numbers to represent the memory landscape of the network. Overall, we tested 35 GRNs, 3,500 configuration models (100 randomized models for each GRN), and 500 RBNs (100 each for networks of size 5, 10, 15, 20, and 25 nodes). We found a non-linear relationship of memory types with network size. Different types of memory begin to appear in RBNs when networks reach 15 nodes in size. Larger networks of 25 nodes have stable quantities of memories and do not increase further. Thus, the structure of the GRN is more important than its mere size for implementing memory. We did not have to search for specific parameters (e.g., frequency) in the input stimulation structure—simple repetition of stimuli was sufficient, suggesting that memory formation may be robust to choices of input timing; however, future work may identify especially effective input patterns.

Interestingly, in the majority of the cases of memory we identified, the input nodes (e.g., CS) received feedback from the network. The establishment of stable states in which the input node is stimulated by the network, long after the real input event has ceased, is similar to a familiar strategy by which neural networks represent states of the world that are not occurring at the moment (acquired memories as “virtual” representations of past events). However, we found 411 cases of memory in which there was no feedback into US or CS from the network, showing that it is possible to achieve dynamical memory without recurrent stimulation back into the input nodes.

Prior work revealed a type of memory in GRNs of the developing vertebrate neural tube and in generic bacterial networks (Herrera-Delgado et al., 2018; Sorek et al., 2013). We found the possibility of other types of memory beyond associative memory, and examined these dynamics broadly across a diverse set of GRNs. Using the data in Cell Collective, we tested 35 GRNs, 100 randomized models of each GRN (3,500 in total) and 500 RBNs (100 of each size 5, 10, 15, 20, and 25). AM was identified in 5 GRNs out of 35 GRNs we tested, and among these GRNs, Aurora Kinase A in Neuroblastoma (vertebrate, cancer category) (Carmena et al., 2009; Dahlhaus et al., 2016), had the highest prevalence of AM. Here, TPX2 (Kufer et al., 2002) appeared as a CS with a variety of genes or processes serving as UCS and R. CD4+ T cell Differentiation and Plasticity (Martinez-Sanchez et al., 2015), B cell differentiation (Méndez and Mendoza, 2016), and Fanconi anemia and checkpoint recovery (Rodríguez et al., 2015) (vertebrate, adult category) have AM. Human gonadal sex determination GRN (vertebrate-embryonic category) also contained AM. Thus AM represents 15% of our GRNs but is available in complex physiological, pathological, and developmental regulatory processes.

We observed that vertebrate GRNs have a much larger amount of memory than invertebrate GRNs (Figure 7A). This may indicate that more complex developmental processes were evolutionarily favored with GRN architectures that exhibit more memory. Interestingly, the gut microbiome GRN is an exception, with significant memory in the invertebrate class; the reason is unknown, but it is likely that memory properties could help microbiota regulate their functions based on patterns in the behavior of the host. Forthcoming work will examine additional GRNs as they become discovered within diverse taxa, to more fully understand the types of memory that exist across the tree of life and the evolutionary significance of their distribution. Likewise, future incorporation of these analyses into artificial embryogeny and evolutionary simulation approaches (Andersen et al., 2009; Basanta et al., 2008; Lowell and Pollack, 2016; Toda et al., 2018) will reveal whether selection for memory capacity potentiates improved developmental complexity and robustness. We further categorized the GRNs into broad "Generic" and "Differentiated" classes (Figure 7B), signifying the rough distinction between networks specific to individual cell types of the body versus more generically applicable or unicellular GRN. With a few exceptions, the broad pattern revealed memory capacity to be more prevalent in GRNs specific to differentiated cell types. However, this conclusion is tempered by the possibility of differential annotation biases in GRN reconstructions of some model systems versus others.

Memories are more common in biological GRNs than in random networks. It should be noted that although there are multiple possible methods to construct randomized networks in addition to our method, we used a method that preserves the major aspects of connectivity while randomizing the Boolean functions, specifically to compare against the null hypothesis that memory is not mediated by the dynamic relationships among the interacting nodes. Our results suggest that memory in a GRN strongly depends on the category of the GRN and the pathological and/or developmental processes in which they are involved, although many more GRNs filling out the space of processes will be useful to have a fuller picture of this relationship. Comparison of each GRN with its randomized configuration models indicated that GRN memory was an outlier compared with its randomized equivalent. Moreover, we found that only in real biological GRNs do different types of memory have distinct correlations between each other. AM is often highly correlated with UM and TM, but not vice versa. Taken together, these analyses reveal several different ways in which biological networks are unique (and reflect richer properties than present simply by virtue of network dynamics in general [Kauffman, 1993, 1995]). Moreover, the specific associations between diverse memory types in biological GRNs form a complex and non-obvious relationship. These findings suggest the possibility that the evolutionary history of real biological organisms contained pressures (direct or indirect) favoring the existence of memory. Thus, an important area for future work is to identify GRN memory phenomena *in vivo* and ascertain their effects on selective advantage in terms of robustness, plasticity, and evolvability.

Numerous opportunities for subsequent work and for the interpretation of puzzling phenomena in biomedicine are suggested by these results. On the computational side, these analyses will next be extended to help understand the historicity of a wide variety of networks—continuous biological models (especially as well-parameterized biological ODE-type GRNs become discovered), protein pathways, and metabolic networks, as well as networks guiding the behavior of designed agents such as soft-body robots (Auerbach and Bongard, 2011; Bongard and Lipson, 2007). The existence of several different memory types could explain phenomena where combinations of drugs produce outcomes that are not predicted by chemical biology, treatments cease working (pharmacoresistance), or well-tolerated compounds begin to have a different (and undesirable) effect with time. Especially in the cancer and microbiome fields, these outcomes are typically thought to be due to population-level selection but could actually result from cellular- or tissue-level memory within individual agents (both host and microbiota). GRN memory may also underlie some of the remarkable variability in drug efficacy and adverse effects that is observed across the population. An individual's response may be partially due to the GRN memories established over a lifetime of unique physiological experiences. Another intriguing potential application of this approach is the exploitation of associative memory to train tissues to respond to an NS to mimic the effects of a potent drug that has too many side effects to use continuously. We will be testing this strategy *in vitro* and *in vivo* at the bench, targeting neuroblastoma and immune cell activation (Figure 5).

It is worth noting that GRNs represented as BNs possess the Markov property, and therefore are "memoryless" in a strict mathematical sense (Markov, 1954). In our work, memories were discovered to be stored by a change in what global attractor the BN is in, which change brought about by external stimuli

(experiences). As the order of interventions matters for which attractor a system ends up in, this is a form of path dependency or hysteresis across gene expression profiles (states of the GRN) (Abraham et al., 2019). Our data and analyses show how this path dependency (in response to interventions) of the node relationships in a GRN can fulfill the classic definitions of memory formation. The network topology determines which nodes can serve as inputs and outputs for a desired type of memory, but no specific structure of the input stimulation is needed besides the relevant repetition mode.

It is essential to understand how much plasticity and historicity can exist without altering the network structure (topology) for the purpose of biomedical applications and for understanding evolutionary change. We demonstrate the phenomenon of non-rewiring memory using a small BN. We show how a form of history-dependent behavior known as "hysteresis" is sufficient for associative memory. Hysteresis, where a recurrent dynamical system shows an opposite response to the same input in the future after passing through a sequence of states (history) steered by external interventions, is not restricted to brains (Cragg and Templerley, 1955). This phenomenon even occurs in ferromagnetic materials where the shape of the magnetic domains in the material depends not only on the applied electric field but also on the shapes of the magnetic domains in the past. As we show in Figure 1, this history could alter the internal state of the system in a way that modulates the effect of a stimulus, which is precisely what associative memory requires.

The type of memory acquisition we observed in these networks has many similarities to learning, which has been shown in a wide variety of neural and aneural systems (Baluška and Levin, 2016). Future work will further highlight parallels between classical models of learning via synaptic plasticity and dynamical learning that can occur in a wide range of substrates including within neurons themselves. It is important to also note that our methods are fully general and could be applied to identify memory in other types of important networks, from contact networks in epidemiology (Perra et al., 2012) to brain networks (Bassett and Sporns, 2017) to drug interaction networks (Barabási et al., 2011). Thus it is likely that the significance of finding trainability in network structures will extend well beyond biology. Overall, the discovery of memories in GRNs is a first step toward merging the approaches of network sciences with a cognitive science-based approach to regulation of complex systems (Manicka and Levin, 2019a; Pezzulo and Levin, 2015). It is likely that the discovery of memory, and perhaps future findings of other aspects of basal cognition in ubiquitous regulatory mechanisms, will provide important insight into the origin, self-regulation, and external control strategies over a broad class of dynamic systems in health sciences and technology.

Limitations of the study

Our analyses were performed on available published models inferred by other groups from primary data (transcriptomic measurements of specific organisms and cell types). Thus, it is possible that conclusions about overall prevalence in memories across different types of networks are affected by ascertainment bias in the construction of available GRNs from the choice of model systems. Our algorithm can be easily applied to revised/updated versions of these GRN models, and to new models that are inferred in future work in the field. Thus, it will be essential to rerun these analyses as new, better GRN models come on line, and to test these novel predictions at the bench. Such functional tests for GRN memory will not only identify interesting biomedical avenues but also serve as a new way to test the quality of GRN models—an additional suite of tests that gauge the fit of the model to predictions of real biological data.

Resource availability

Lead contact

michael.levin@tufts.edu.

Materials availability

n/a.

Data and code availability

All numerical results are available upon request. Code is not yet public due to intellectual property restrictions; contact corresponding author with requests.

METHODS

All methods can be found in the accompanying [Transparent methods supplemental file](#).

SUPPLEMENTAL INFORMATION

Supplemental information can be found online at <https://doi.org/10.1016/j.isci.2021.102131>.

ACKNOWLEDGMENTS

We thank Richard Chechile and Charles Abramson for helpful discussions, Anna Kane, Megan Sperry, and Julia Poirier for useful comments on the manuscript, and Jeremy Guay of Peregrine Creative and Luba Levin for assistance with the graphical abstract. We gratefully acknowledge support by an Allen Discovery Center award from the Paul G. Allen Frontiers Group (No. 12171) and the Templeton World Charity Foundation (No. TWCF0089/AB55).

AUTHOR CONTRIBUTIONS

M.L. conceived of the project and overall approach. S.B. wrote the code and performed the experiments. S.B., S.M., E.H., and M.L. all contributed to the data analysis and experimental design, and wrote the paper.

DECLARATION OF INTERESTS

The authors declare no competing interests.

Received: August 17, 2020

Revised: December 9, 2020

Accepted: January 26, 2021

Published: March 19, 2021

REFERENCES

- Abraham, W.C., Jones, O.D., and Glanzman, D.L. (2019). Is plasticity of synapses the mechanism of long-term memory storage? *NPJ Sci. Learn.* 4, 1–10.
- Albert, I., Thakar, J., Li, S., Zhang, R., and Albert, R. (2008). Boolean network simulations for life scientists. *Source Code Biol. Med.* 3, 16.
- Albert, R., and Thakar, J. (2014). Boolean modeling: a logic-based dynamic approach for understanding signaling and regulatory networks and for making useful predictions. *Wiley Interdiscip. Rev. Syst. Biol. Med.* 6, 353–369.
- Albert, R.e. (2004). Boolean modeling of genetic regulatory networks. In *Complex Networks Lecture Notes in Physics*, 650, E. Ben-Naim, H. Frauenfelder, and Z. Toroczkai, eds (Springer), pp. 459–481.
- Alvarez-Buylla, E.R., Balleza, E., Benitez, M., Espinosa-Soto, C., and Padilla-Longoria, P. (2008). Gene regulatory network models: a dynamic and integrative approach to development. *SEB Exp. Biol. Ser.* 61, 113–139.
- Andersen, T., Newman, R., and Otter, T. (2009). Shape homeostasis in virtual embryos. *Artif. Life* 15, 161–183.
- Auerbach, J.E., and Bongard, J.C. (2011). Evolving complete robots with CPPN-neat: the utility of recurrent connections. In *Gecco-2011: Proceedings of the 13th Annual Genetic and Evolutionary Computation Conference* (ACM Press), pp. 1475–1482.
- Bacchus, W., Aubel, D., and Fussenegger, M. (2013). Biomedically relevant circuit-design strategies in mammalian synthetic biology. *Mol. Syst. Biol.* 9, 691.
- Baluška, F., and Levin, M. (2016). On having No head: cognition throughout biological systems. *Front. Psychol.* 7, 902.
- Banerjee, K. (2015). Dynamic memory of a single voltage-gated potassium ion channel: Astrostoachastic nonequilibrium thermodynamic analysis. *J. Chem. Phys.* 142, 185101.
- Barabási, A.-L., Gulbahce, N., and Loscalzo, J. (2011). Network medicine: a network-based approach to human disease. *Nat. Rev. Genet.* 12, 56–68.
- Barberis, M., and Helikar, T. (2019). Logical Modeling of Cellular Processes: From Software Development to Network Dynamics (Frontiers media SA).
- Basanta, D., Miodownik, M., and Baum, B. (2008). The evolution of robust development and homeostasis in artificial organisms. *PLoS Comput. Biol.* 4, e1000030.
- Bassett, D.S., and Sporns, O. (2017). Network neuroscience. *Nat. Neurosci.* 20, 353.
- Blackiston, D.J., and Levin, M. (2013). Ectopic eyes outside the head in *Xenopus* tadpoles provide sensory data for light-mediated learning. *J. Exp. Biol.* 216, 1031–1040.
- Blais, A., and Dynlacht, B.D. (2005). Constructing transcriptional regulatory networks. *Genes Dev.* 19, 1499–1511.
- Bongard, J., and Lipson, H. (2007). Automated reverse engineering of nonlinear dynamical systems. *Proc. Natl. Acad. Sci. U S A* 104, 9943–9948.
- Bornholdt, S., and Kauffman, S. (2019). Ensembles, dynamics, and cell types: revisiting the statistical mechanics perspective on cellular regulation. *J. Theor. Biol.* 467, 15–22.
- Carmena, M., Ruchaud, S., and Earnshaw, W.C. (2009). Making the Auroras glow: regulation of Aurora A and B kinase function by interacting proteins. *Curr. Opin. Cell Biol.* 21, 796–805.
- Chechile, R.A. (2018). *Analyzing Memory : The Formation, Retention, and Measurement of Memory* (The MIT Press).
- Corre, G., Stockholm, D., Arnaud, O., Kaneko, G., Vinuelas, J., Yamagata, Y., Neildez-Nguyen, T.M., Kupiec, J.J., Beslon, G., Gandrillon, O., et al. (2014). Stochastic fluctuations and distributed control of gene expression impact cellular memory. *PLoS One* 9, e115574.
- Cragg, B.G., and Temperley, H.N. (1955). Memory: the analogy with ferromagnetic hysteresis. *Brain* 78, 304–316.
- Crommelinck, M., Feltz, B., and Goujon, P. (2006). *Self-organization and Emergence in Life Sciences* (Springer).
- Dahlhaus, M., Burkowski, A., Hertwig, F., Mussel, C., Volland, R., Fischer, M., Debatin, K.M., Kestler, H.A., and Beltinger, C. (2016). Boolean modeling identifies Greatwall/MASTL as an important regulator in the AURKA network of neuroblastoma. *Cancer Lett.* 371, 79–89.
- Daoudal, G., and Debanne, D. (2003). Long-term plasticity of intrinsic excitability: learning rules and mechanisms. *Learn. Mem.* 10, 456–465.
- Davidson, E.H. (2010). Emerging properties of animal gene regulatory networks. *Nature* 468, 911–920.

- De Jong, H. (2002). Modeling and simulation of genetic regulatory systems: a literature review. *J. Comput. Biol.* 9, 67–103.
- Debanne, D., Daoudal, G., Sourdet, V., and Russier, M. (2003). Brain plasticity and ion channels. *J. Physiol. Paris* 97, 403–414.
- Delgado, F.M., and Gómez-Vela, F. (2019). Computational methods for Gene Regulatory Networks reconstruction and analysis: a review. *Artif. Intell. Med.* 95, 133–145.
- Demongeot, J., Hasgui, H., and Thellier, M. (2019). Memory in plants: boolean modeling of the learning and store/recall memory functions in response to environmental stimuli. *J. Theor. Biol.* 467, 123–133.
- Deritei, D., Rozum, J., Regan, E.R., and Albert, R. (2019). A feedback loop of conditionally stable circuits drives the cell cycle from checkpoint to checkpoint. *Sci. Rep.* 9, 1–19.
- Durant, F., Morokuma, J., Fields, C., Williams, K., Adams, D.S., and Levin, M. (2017). Long-term, stochastic editing of regenerative anatomy via targeting endogenous bioelectric gradients. *Biophys. J.* 112, 2231–2243.
- Durso, F.T., and Nickerson, R.S. (1999). *Handbook of Applied Cognition* (Wiley).
- Eduati, F., Doldà-Martelli, V., Klinger, B., Cokelaer, T., Sieber, A., Kogera, F., Dorel, M., Garnett, M.J., Blüthgen, N., and Saez-Rodriguez, J. (2017). Drug resistance mechanisms in colorectal cancer dissected with cell type-specific dynamic logic models. *Cancer Res.* 77, 3364–3375.
- Emmons-Bell, M., Durant, F., Tung, A., Pietak, A., Miller, K., Kane, A., Martyniuk, C.J., Davidian, D., Morokuma, J., and Levin, M. (2019). Regenerative adaptation to electrochemical perturbation in planaria: a molecular analysis of physiological plasticity. *iScience* 22, 147–165.
- Fazilaty, H., Rago, L., Kass Youssef, K., Ocana, O.H., García-Asencio, F., Arcas, A., Galceran, J., and Nieto, M.A. (2019). A gene regulatory network to control EMT programs in development and disease. *Nat. Commun.* 10, 5115.
- Fernando, C.T., Liekens, A.M., Bingle, L.E., Beck, C., Lenser, T., Stekel, D.J., and Rowe, J.E. (2009). Molecular circuits for associative learning in single-celled organisms. *J. R. Soc. Interf.* 6, 463–469.
- Frey, N., Bodmer, M., Bircher, A., Jick, S.S., Meier, C.R., and Spoendlin, J. (2019). Stevens-johnson syndrome and toxic epidermal necrolysis in association with commonly prescribed drugs in outpatient care other than anti-epileptic drugs and antibiotics: a population-based case-control study. *Drug Saf.* 42, 55–66.
- Gallaher, J., Bier, M., and van Heukelom, J.S. (2010). First order phase transition and hysteresis in a cell's maintenance of the membrane potential-An essential role for the inward potassium rectifiers. *Biosystems* 101, 149–155.
- Gant, W.H. (1974). Autokinesis, schizokinesis, centrokinesis and organ-system responsibility: concepts and definition. *Pavlov. J. Biol. Sci.* 9, 187–191.
- Gant, W.H. (1981). Organ-system responsibility, schizokinesis, and autokinesis in behavior. *Pavlov. J. Biol. Sci.* 16, 64–66.
- Geukes Foppen, R.J., van Mil, H.G., and van Heukelom, J.S. (2002). Effects of chloride transport on bistable behaviour of the membrane potential in mouse skeletal muscle. *J. Physiol.* 542, 181–191.
- Goel, P., and Mehta, A. (2013). Learning theories reveal loss of pancreatic electrical connectivity in diabetes as an adaptive response. *PLoS One* 8, e70366.
- Helikar, T., Kowal, B., McClenathan, S., Bruckner, M., Rowley, T., Madrahimov, A., Wicks, B., Shrestha, M., Limbu, K., and Rogers, J.A. (2012). The cell collective: toward an open and collaborative approach to systems biology. *BMC Syst. Biol.* 6, 96.
- Herrera-Delgado, E., Perez-Carrasco, R., Briscoe, J., and Sollich, P. (2018). Memory functions reveal structural properties of gene regulatory networks. *PLoS Comput. Biol.* 14, e1006003.
- Hoffmann, H. (2015). violin.m - Simple Violin Plot Using Matlab Default Kernel Density Estimation (INRES (University of Bonn)). hoffmann@uni-bonn.de.
- Huang, S., Eichler, G., Bar-Yam, Y., and Ingber, D.E. (2005). Cell fates as high-dimensional attractor states of a complex gene regulatory network. *Phys. Rev. Lett.* 94, 128701.
- Izquierdo, E.J., Eduardo, Harvey, Inman, Beer, and Randall, D. (2008). Associative learning on a continuum in evolved dynamical neural networks. *Adapt. Behav.* 16, 361–384.
- Kandel, E.R., Dudai, Y., and Mayford, M.R. (2014). The molecular and systems biology of memory. *Cell* 157, 163–186.
- Karsenti, E. (2008). Self-organization in cell biology: a brief history. *Nat. Rev. Mol. Cell Biol.* 9, 255–262.
- Kauffman, S.A. (1969). Metabolic stability and epigenesis in randomly constructed genetic nets. *J. Theor. Biol.* 22, 437–467.
- Kauffman, S.A. (1993). *The Origins of Order : Self Organization and Selection in Evolution* (Oxford University Press).
- Kauffman, S.A. (1995). *At Home in the Universe : The Search for Laws of Self-Organization and Complexity* (Oxford University Press).
- Kauffman, S.A., and Strohman, R.C. (1994). *The Origins of Order: Self Organization and Selection in Evolution* (Oxford university press).
- Kohonen, T. (2012). *Self-organization and Associative Memory*, 8 (Springer Science & Business Media).
- Kufer, T.A., Sillje, H.H., Korner, R., Gruss, O.J., Meraldi, P., and Nigg, E.A. (2002). Human TPX2 is required for targeting Aurora-A kinase to the spindle. *J. Cell Biol.* 158, 617–623.
- Lähdesmäki, H., Shmulevich, I., and Yli-Harja, O. (2003). On learning gene regulatory networks under the Boolean network model. *Mach. Learn.* 52, 147–167.
- Law, R., and Levin, M. (2015). Bioelectric memory: modeling resting potential bistability in amphibian embryos and mammalian cells. *Theor. Biol. Med. Model.* 12, 22.
- Lee, T.I., and Young, R.A. (2013). Transcriptional regulation and its misregulation in disease. *Cell* 152, 1237–1251.
- Levin, M. (2014). Endogenous bioelectrical networks store non-genetic patterning information during development and regeneration. *J. Physiol.* 592, 2295–2305.
- Levine, J.H., Lin, Y., and Elowitz, M.B. (2013). Functional roles of pulsing in genetic circuits. *Science* 342, 1193–1200.
- Lobo, D., Solano, M., Bubenik, G.A., and Levin, M. (2014). A linear-encoding model explains the variability of the target morphology in regeneration. *J. R. Soc. Interf.* 11, 20130918.
- Lowell, J., and Pollack, J. (2016). Developmental encodings promote the emergence of hierarchical modularity. In *Proceedings of the Artificial Life Conference 2016* (MIT Press), pp. 344–351.
- Macia, J., Vidiella, B., and Solé, R.V. (2017). Synthetic associative learning in engineered multicellular consortia. *J. R. Soc. Interf.* 14, 20170158.
- Macneil, L.T., and Walhout, A.J. (2011). Gene regulatory networks and the role of robustness and stochasticity in the control of gene expression. *Genome Res.* 21, 645–657.
- Manicka, S., and Levin, M. (2019a). The Cognitive Lens: a primer on conceptual tools for analysing information processing in developmental and regenerative morphogenesis. *Philos. Trans. R. Soc. Lond. B Biol. Sci.* 374, 20180369.
- Manicka, S., and Levin, M. (2019b). Modeling somatic computation with non-neural bioelectric networks. *Sci. Rep.* 9, 18612.
- Markov, A.A. (1954). *The Theory of Algorithms*, 42 (Trudy Matematicheskogo Instituta Imeni VA. Steklova), pp. 3–375.
- Marques-Pita, M., and Rocha, L.M. (2013). Canalization and control in automata networks: body segmentation in *Drosophila melanogaster*. *PLoS One* 8, e55946.
- Martin, S., Zhang, Z., Martino, A., and Faulon, J.-L. (2007). Boolean dynamics of genetic regulatory networks inferred from microarray time series data. *Bioinformatics* 23, 866–874.
- Martinez-Sánchez, M.E., Mendoza, L., Villarreal, C., and Alvarez-Buylla, E.R. (2015). A minimal regulatory network of extrinsic and intrinsic factors recovers observed patterns of CD4+ T cell differentiation and plasticity. *PLoS Comput. Biol.* 11, e1004324.
- McGregor, S., Vasas, V., Husbands, P., and Fernando, C. (2012). Evolution of associative learning in chemical networks. *PLoS Comput. Biol.* 8, e1002739.
- Méndez, A., and Mendoza, L. (2016). A network model to describe the terminal differentiation of B cells. *PLoS Comput. Biol.* 12, e1004696.

- Nashun, B., Hill, P.W., and Hajkova, P. (2015). Reprogramming of cell fate: epigenetic memory and the erasure of memories past. *EMBO J.* 34, 1296–1308.
- Palm, G. (1980). On associative memory. *Biol. Cybern.* 36, 19–31.
- Perra, N., Gonçalves, B., Pastor-Satorras, R., and Vespignani, A. (2012). Activity driven modeling of time varying networks. *Sci. Rep.* 2, 469.
- Peter, I.S., and Davidson, E.H. (2011). Evolution of gene regulatory networks controlling body plan development. *Cell* 144, 970–985.
- Pezzulo, G., and Levin, M. (2015). Re-membering the body: applications of computational neuroscience to the top-down control of regeneration of limbs and other complex organs. *Integr. Biol. (Camb)* 7, 1487–1517.
- Pezzulo, G., and Levin, M. (2016). Top-down models in biology: explanation and control of complex living systems above the molecular level. *J. R. Soc. Interface* 13, 20160555.
- Qin, G., Yang, L., Ma, Y., Liu, J., and Huo, Q. (2019). The exploration of disease-specific gene regulatory networks in esophageal carcinoma and stomach adenocarcinoma. *BMC Bioinformatics* 20, 717.
- Quintin, J., Cheng, S.C., van der Meer, J.W., and Netea, M.G. (2014). Innate immune memory: towards a better understanding of host defense mechanisms. *Curr. Opin. Immunol.* 29C, 1–7.
- Rescorla, R.A. (1967). Pavlovian conditioning and its proper control procedures. *Psychol. Rev.* 74, 71.
- Rodríguez, A., Torres, L., Juárez, U., Sosa, D., Azpeitia, E., García-de Teresa, B., Cortés, E., Ortiz, R., Salazar, A.M., and Ostrosky-Wegman, P. (2015). Fanconi anemia cells with unrepaired DNA damage activate components of the checkpoint recovery process. *Theor. Biol. Med. Model.* 12, 19.
- Ryan, T.J., Roy, D.S., Pignatelli, M., Arons, A., and Tonegawa, S. (2015). Engram cells retain memory under retrograde amnesia. *Science* 348, 1007–1013.
- Saez-Rodriguez, J., Alexopoulos, L.G., Epperlein, J., Samaga, R., Lauffenburger, D.A., Klamt, S., and Sorger, P.K. (2009). Discrete logic modelling as a means to link protein signalling networks with functional analysis of mammalian signal transduction. *Mol. Syst. Biol.* 5, 331.
- Samal, A., and Jain, S. (2008). The regulatory network of *E. coli* metabolism as a Boolean dynamical system exhibits both homeostasis and flexibility of response. *BMC Syst. Biol.* 2, 21.
- Schlitt, T., and Brazma, A. (2007). Current approaches to gene regulatory network modelling. *BMC bioinformatics* 8, S9.
- Schreier, H.I., Soen, Y., and Brenner, N. (2017). Exploratory adaptation in large random networks. *Nat. Commun.* 8, 14826.
- Science, A.A.f.t.A.o. (2003). Maturing from memory. *Sci. Signal.* 2003, tw462.
- Sherrington, D., and Wong, K. (1989). Random boolean networks for autoassociative memory. *Phys. Rep.* 184, 293–299.
- Sherrington, D., and Wong, K. (1990). Random Boolean Networks for Autoassociative Memory: Optimization and Sequential Learning. In *Statistical Mechanics of Neural Networks* (Springer), pp. 467–473.
- Sible, J.C. (2003). Thanks for the memory. *Nature* 426, 392–393.
- Singh, A.J., Ramsey, S.A., Filtz, T.M., and Kioussi, C. (2018). Differential gene regulatory networks in development and disease. *Cell. Mol. Life Sci.* 75, 1013–1025.
- Snipas, M., Kraujalis, T., Paulauskas, N., Maciunas, K., and Bukauskas, F.F. (2016). Stochastic model of gap junctions exhibiting rectification and multiple closed states of slow gates. *Biophys. J.* 110, 1322–1333.
- Soen, Y., Knafo, M., and Elgart, M. (2015). A principle of organization which facilitates broad Lamarckian-like adaptations by improvisation. *Biol. Direct* 10, 68.
- Sorek, M., Balaban, N.Q., and Loewenstein, Y. (2013). Stochasticity, bistability and the wisdom of crowds: a model for associative learning in genetic regulatory networks. *PLoS Comput. Biol.* 9, e1003179.
- Stockwell, S.R., Landry, C.R., and Rifkin, S.A. (2015). The yeast galactose network as a quantitative model for cellular memory. *Mol. Biosyst.* 11, 28–37.
- Sullivan, K.G., Emmons-Bell, M., and Levin, M. (2016). Physiological inputs regulate species-specific anatomy during embryogenesis and regeneration. *Commun. Integr. Biol.* 9, e1192733.
- Szabó, Á., Vattay, G., and Kondor, D. (2012). A cell signaling model as a trainable neural nanonetwok. *Nano Commun. Networks* 3, 57–64.
- Tagkopoulos, I., Liu, Y.C., and Tavazoie, S. (2008). Predictive behavior within microbial genetic networks. *Science* 320, 1313–1317.
- Thomas, P., Popović, N., and Grima, R. (2014). Phenotypic switching in gene regulatory networks. *Proc. Natl. Acad. Sci. U S A* 111, 6994–6999.
- Thomas, R. (1973). Boolean formalization of genetic control circuits. *J. Theor. Biol.* 42, 563–585.
- Toda, S., Blauch, L.R., Tang, S.K.Y., Morsut, L., and Lim, W.A. (2018). Programming self-organizing multicellular structures with synthetic cell-cell signaling. *Science* 361, 156–162.
- Turner, C.H., Robling, A.G., Duncan, R.L., and Burr, D.B. (2002). Do bone cells behave like a neuronal network? *Calcif. Tissue Int.* 70, 435–442.
- Tyson, J.J., Laometsachit, T., and Kraikivski, P. (2019). Modeling the dynamic behavior of biochemical regulatory networks. *J. Theor. Biol.* 462, 514–527.
- Urrios, A., Macia, J., Manzoni, R., Conde, N., Bonfatti, A., de Nadal, E.I., Posas, F., and Sole, R. (2016). A synthetic multicellular memory device. *ACS Synth. Biol.* 5, 862–873.
- Wang, R.S., Saadatpour, A., and Albert, R. (2012). Boolean modeling in systems biology: an overview of methodology and applications. *Phys. Biol.* 9, 055001.
- Watson, R.A., Buckley, C.L., Mills, R., and Davies, A. (2010). Associative memory in gene regulation networks. In *Artificial Life Conference XII* (Odense, Denmark) (MIT Press), pp. 659–666.
- Watson, R.A., Mills, R., and Buckley, C.L. (2011). Global adaptation in networks of selfish components: emergent associative memory at the system scale. *Artif. Life* 17, 147–166.
- Watson, R.A., Wagner, G.P., Pavlicev, M., Weinreich, D.M., and Mills, R. (2014). The evolution of phenotypic correlations and "developmental memory". *Evolution* 68, 1124–1138.
- Weitz, M., and Simmel, F.C. (2012). Synthetic in vitro transcription circuits. *Transcription* 3, 87–91.
- Wery, M., Dameron, O., Nicolas, J., Remy, E., and Siegel, A. (2019). Formalizing and enriching phenotype signatures using Boolean networks. *J. Theor. Biol.* 467, 66–79.
- Xiong, W., and Ferrell, J.E. (2003). A positive-feedback-based bistable 'memory module' that governs a cell fate decision. *Nature* 426, 460–465.
- Yamauchi, B.M., and Beer, R. (1994). Sequential Behavior and Learning in evolved dynamical neural networks. *Adapt. Behav.* 2, 219–246.
- Zagorski, M., Tabata, Y., Brandenberg, N., Lutolf, M.P., Tkacik, G., Bollenbach, T., Briscoe, J., and Kicheva, A. (2017). Decoding of position in the developing neural tube from antiparallel morphogen gradients. *Science* 356, 1379–1383.
- Zanudo, J.G., and Albert, R. (2015). Cell fate reprogramming by control of intracellular network dynamics. *PLoS Comput. Biol.* 11, e1004193.
- Zañudo, J.G.T., Yang, G., and Albert, R. (2017). Structure-based control of complex networks with nonlinear dynamics. *Proc. Natl. Acad. Sci. U S A* 114, 7234–7239.
- Zediak, V.P., Wherry, E.J., and Berger, S.L. (2011). The contribution of epigenetic memory to immunologic memory. *Curr. Opin. Genet. Dev.* 21, 154–159.

Supplemental information

**Gene regulatory networks exhibit several
kinds of memory: Quantification of memory
in biological and random transcriptional networks**

Surama Biswas, Santosh Manicka, Erik Hoel, and Michael Levin

Transparent Methods

Biological GRN models

We used a set of 35 models of GRNs downloaded from an online repository called *Cell Collective* (Helikar et al., 2012), consisting of a maximum of 25 nodes each. Each model is defined as a standard Boolean Network (BN) (Herrmann et al., 2012): a discrete dynamical system whose nodes represent the components of the system (e.g., genes or proteins) that can be in one of two states, namely 1 (ON) or 0 (OFF), and whose edges represent the regulatory interactions (activation/repression) among the nodes, dictating their states (Kauffman et al., 2003). The state of a BN is represented as a vector of the individual gene states, updated synchronously in discrete time-steps: the state of each gene at time $t + 1$ is determined by a Boolean function of the states of its input genes at time t (Shmulevich and Kauffman, 2004). The BNs in the *Cell Collective* database are defined using only the elementary Boolean functions, namely AND, OR and NOT, since any Boolean function can be expressed using some combination of these elementary operators. A BN is simulated by initializing it with some state, then updating it to obtain the next state, and so on, for a specified number of time-steps. When a BN is simulated for a long enough time, it reaches an attractor state. An attractor may consist of a single BN state, known as a “point attractor”, or may consist of a set of states that the network cycles through, known as a “cyclic attractor.” A BN can have multiple attractors, and different inputs may lead to different attractors (Graudenzi et al., 2011; Groß et al., 2019; Mochizuki et al., 2013; Naldi et al., 2018; Serra et al., 2007; Shmulevich and Dougherty, 2010; Shmulevich and Kauffman, 2004; Veliz-Cuba et al., 2014; Xiao, 2009). In this work, we compute the memory profile of BNs in a manner that pays attention to its attractor states in order to avoid the effects of the transient dynamics on the analyses. This imposes a limitation on the size of networks considered here because the larger the network, the longer it takes to reach an attractor. This *transient length* to reach an attractor depends on the *Network Size* (the number of nodes in the network) and the *Edge Density* defined as (Number of edges / Total number of possible edges). We found that the transient length (Supplement 14) rises exponentially above 500 time-steps (a practical limit that we chose for this work) for networks of size larger than 25 with a biologically realistic edge density of 10% (Supplement 15). As a result, we restricted ourselves to analysis of BNs of size ≤ 25 to be able to exhaustively analyze all our networks.

Synthetic GRN models for comparison

To evaluate the significance of the memory profiles of the biological GRN models, we generated synthetic Null models for comparison: 1) a set of 3500 BNs obtained by randomizing each GRN 100 times, known as “configuration models”; and 2) a set of 500 random Boolean networks (RBN).

We generated a set of 100 configuration models for each one of the 35 biological GRN models. There are many ways to generate the configuration (Null) models, depending on the null hypothesis that one wishes to consider (Zhai et al., 2018). Since our principal motivation is the idea that memory in GRNs may be mediated by the dynamic relationships among the node's mechanisms, our null hypothesis is therefore that those dynamic relationships don't play a role in mediating memory-related phenomena but are entirely governed by things like edge degree. Therefore, in generating each configuration model we kept the number of nodes and the indegree distribution the same as the original GRN, while randomizing only the inputs to the nodes and the associated Boolean functions. That is, each node in the configuration model has the same number of inputs, but the actual input nodes will be different compared to the original model. Similarly, each Boolean function in the configuration model has the same number of inputs as the original but the Boolean operators are randomly chosen from the set of elementary operators (AND, OR, NOT).

To determine how the memory properties of networks vary with network size in general, we generated five sets of 100 RBNs each, of size 5, 10, 15, 20 and 25 nodes respectively. The edge density was set to $\max(10\% \text{ of } N^2, N - 1)$, as the average edge density of the biological GRNs was found to be $\sim 10\%$. Unlike the configuration models, we generated an RBN by first randomly choosing unique source-target node pairs and assigning a directed edge between them such that the total number of edges satisfied the specified edge density, and then assigning random Boolean functions to each node. We generated a random Boolean function for a given node as follows. First, we considered the inputs of the node X that may consist of just one input (X itself or some other node,) or more than one input. In the case of the former, the Boolean function may take one of the following forms: ' $X = X$ ', ' $X = Y$ ' or ' $X = \sim Y$ ', where ' \sim ' represents logical NOT (invert) operation. If there are two or more inputs, such as (Y, Z) , the Boolean function may take one of the following forms: $(Y \otimes Z)$, $(\sim Y \otimes Z)$, $(Y \otimes \sim Z)$ or $(\sim Y \otimes \sim Z)$, where \otimes represents a Boolean operator randomly chosen from the list of Boolean operators (AND, OR and XOR). For more than two inputs, the Boolean functions would simply be larger compositions of the above. We then randomly applied NOT operation in the final or intermediate stages of the equation so that 50% of the nodes were affected.

Synthetic GRN models for illustration

To illustrate the phenomenon of memory formation in BNs, we generated 10000 minimal RBNs consisting of 2 and 3 nodes (Figure 5). The process of making the minimal models was same as that of making RBNs except the fact that here we selected a higher edge density randomly in [50, 100]. As we are interested here finding memory in the small networks where the number of nodes is few (2/3), a denser topology is required to produce memory. We first investigated the minimum number of nodes required to form a certain type of memory. In the case of UCS based memory, the minimum requirement was 2 (UCS and R); for all other types of memory it was 3 (UCS, NS/CS, and R). We then

fixed the edge density at a random percentage between 50 and 100. We evaluated memory and took as minimal the one which had the fewest edges.

Memory detection

We defined different types of memories, characterized by a specific number and timing of the stimuli, as described below. For each network, we looked for possible memories by considering all possible choices of nodes to serve as inputs or outputs in a training assay. We exhaustively considered all choices of nodes subject to the requirement that any node can only be a valid UCS if it triggers R prior to training, and any node can serve as a NS if it does not trigger R prior to training. In 3 cases, (*Arabidopsis thaliana* Cell Cycle, Iron acquisition and oxidative stress response in *aspergillus fumigatus* and Budding Yeast Cell Cycle 2009), we could not find any combinations matching this feasibility condition and thus considered the amount of “no memory” to be 100%. The set of all feasible stimulus-response combinations is a subset of all possible combinations, the cardinality of which is given by $P(N, 3) = \frac{N!}{(N-3)!}$. We compute a memory profile for each feasible combination by passing it through a series of detection steps (Figure 3). We first let the BN settle on an attractor by initiating it with a state consisting of all “off” and simulating it for 500 time-steps.

Then, we evaluated the memory of each network, given a choice of nodes as CS, UCS, and R via a sequence of steps picked from the following general recipe (the specific steps followed depends on the type of the memory being evaluated): 1) choose a stimulus set; 2) flip the state of the stimuli and fix them in that state, referred to as *clamping* (we did not let other genes to alter the state of UCS and all equations associated with different genes and UCS get the clamped value of UCS); 3) simulate the BN for M time-steps; 4) record the state of R compared to its state prior to the clamping step; 5) unclamp the stimuli (allow them to update states), referred to as *relaxation*; 6) simulate the BN for M time-steps; 7) record the state of R compared to its state prior to relaxation; 8) choose a different stimulus set; 9) flip and clamp the stimuli; 10) simulate the BN for M time-steps; 11) record the state of R compared to its state prior to the clamping step 9; 12) relax the network; and 13) record the state of R . We deemed a given stimulus-response combination as having elicited a specific type of memory if it satisfies the associated set of conditions:

- i) *UCS Based Memory (UM)*: choose the stimulus set consisting of in step 1, verify that R has flipped in step 3, and finally verify that R has *not* flipped in step 7. UM captures the idea that R may permanently remember changes in the activity of UCS.
- ii) *Pairing Memory (PM)*: choose the stimulus set consisting of {UCS, NS} in step 1, verify that R has flipped in step 3, and finally verify that R has *not* flipped in step 7. PM captures the idea that R may permanently remember changes in the joint

- activities of UCS and NS. Even though the detection of PM is like AM, there are crucial differences (see AM definition below).
- iii) *Transfer Memory* (TM): choose the stimulus set consisting of {UCS} in step 1, verify that R has flipped in step 3, choose the stimulus set consisting of {NS} in step 8, and finally verify that R has flipped in step 11. TM captures the possibility that even though NS could not flip R initially, it may be able to do so after activating UCS, effectively transforming NS into CS.
 - iv) *Associative Memory* (AM): choose the stimulus set consisting of {UCS, NS} in step 1, verify that R has flipped in step 3, choose the stimulus set consisting of {NS} in step 8, and finally verify that R has flipped in step 11. AM describes classical conditioning: after successful pairing of UCS and current NS, the NS is conditioned to become CS. This causes the NS to become CS and can be able to trigger R. In other words, we call it an AM if after successful pairing, NS can flip R.
 - a. *Long Recall Associative Memory* (LRAM): Following the AM steps, verify that R has *not* flipped in step 13 compared to its state prior to the relaxation step 12. LRAM captures the idea that R may permanently remember changes to the activity of CS.
 - b. *Short Recall Associative Memory* (SRAM): Following the AM steps, verify that R has flipped in step 13 compared to its state prior to the relaxation step 12. SRAM captures the idea that R may only transiently remember changes to the activity of CS.
 - v) *Consolidation Memory* (CM): choose the stimulus set consisting of {UCS, NS} in step 1, verify that R has flipped in step 3, choose the stimulus set consisting of {NS} in step 8, verify that R has *not* flipped in step 11, and finally verify that R has flipped compared to its state prior to the clamping step 9. CM captures the idea that even though associative conditioning may not immediately turn NS into CS, it may do so after relaxing the BN.

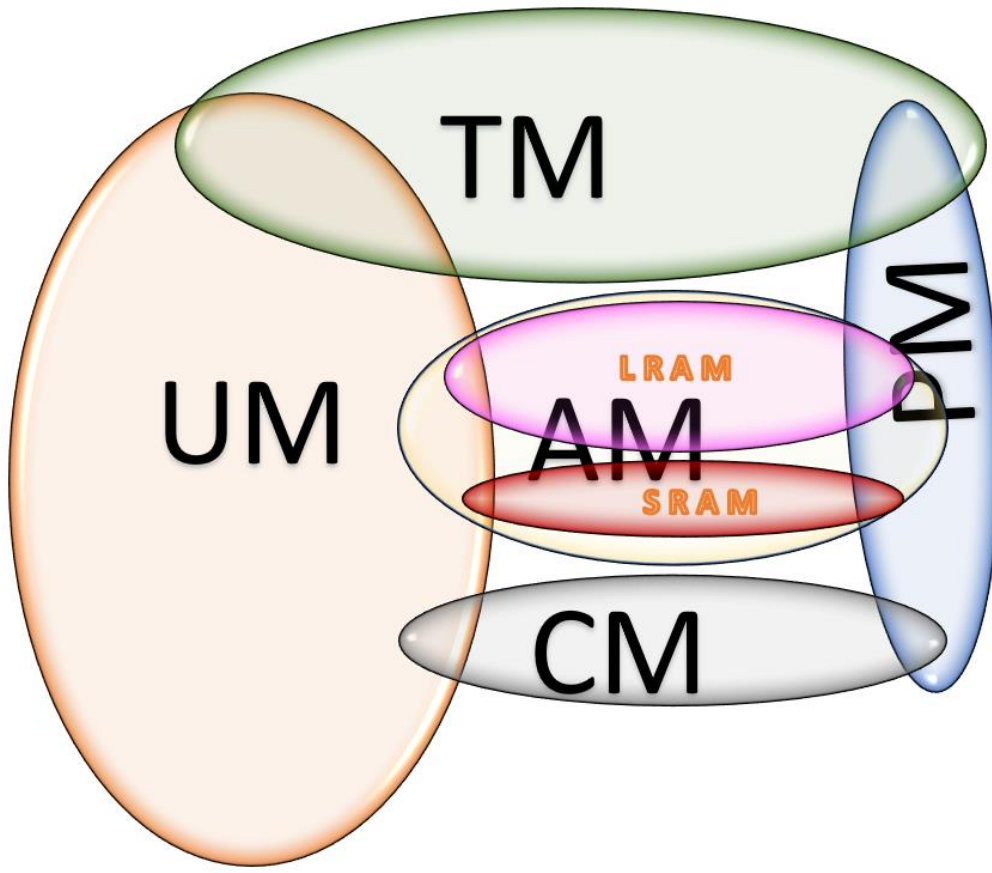
Note that UM and PM are mutually exclusive, as are TM and {AM, CM} (see Figures 2,3 for details).

After confirmation of each case of Transfer, Associative and Consolidation memory, we checked whether the change in the property of NS in inducing R is permanent. We deactivated the CS to check if R is also deactivated; again we activated CS to see if R is triggered back, and continued the activation/deactivation process 20 times to see if causality between NS and R is stable. If stable, we called it second order memory.

Mathematically, in an N node GRN, there may be P_N^3 such combinations. Here, we considered the current node as R if the R is stable over a certain period called *Constancy Length* during the relaxation phase of the network (see Supplement 16). We coded the methodology in MATLAB 2019a.

Supplements

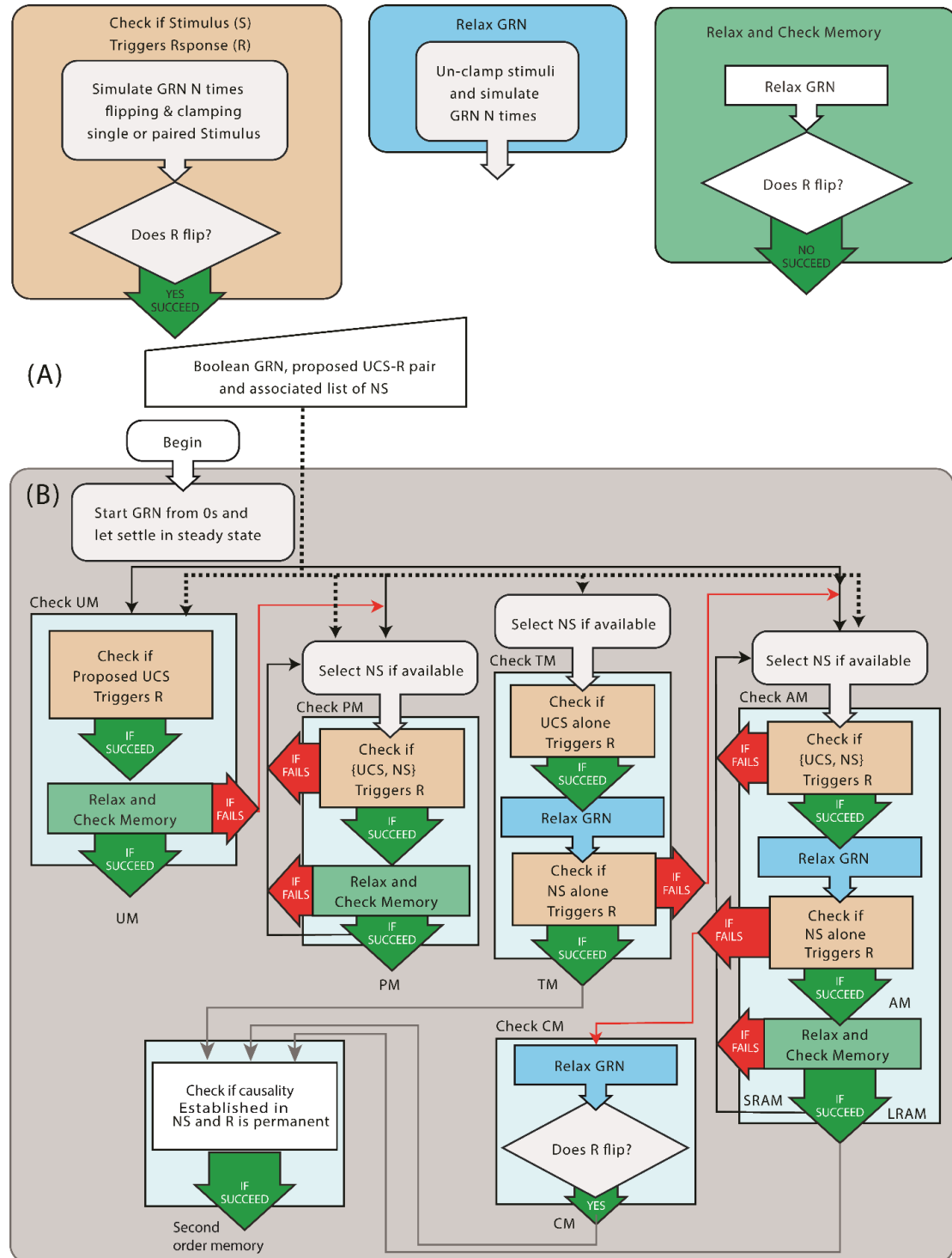
Supplemental Figure 1: Definition of and functional relationship among the different memory types [This item relates to Figure 2]



UM: UCS Based Memory	PM: Pairing Memory	TM: Transfer Memory
AM: Associative Memory	LRAM: Long Recall AM	SRAM: Short Recall AM
CM: Consolidation Memory	NM: No Memory	

Legend: The definition and abbreviations of the defined memory types are as follows. UCS Based Memory UM: R retains the activation by UCS after UCS deactivated. Pairing Memory (PM): R retains the repetitive activation by {UCS, NS} pair even after their deactivation. Transfer Memory (TM): activation by UCS alone (not pairing) converts NS to CS. Associative Memory (AM): paired activation of {UCS, NS}, converts NS to CS. Long Recall AM (LRAM): this conversion of NS to CS is permanent. Short Recall AM (SRAM): the conversion is temporary (the association is lost). Consolidation Memory (CM): the pairing of {UCS, NS} does not immediately turn NS into CS but eventually does so after an elapsed time. The overlap/hierarchy of the ovals represents the relationship between the different types and subtypes of memory.

Supplemental Figure 2: Flowchart of Memory Evaluation [This item relates to Figure 2]



Legend: The computational procedures for our evaluation of five kinds of memories are shown here, namely, UM, PM, TM, AM and CM. We consider each of the two sub-

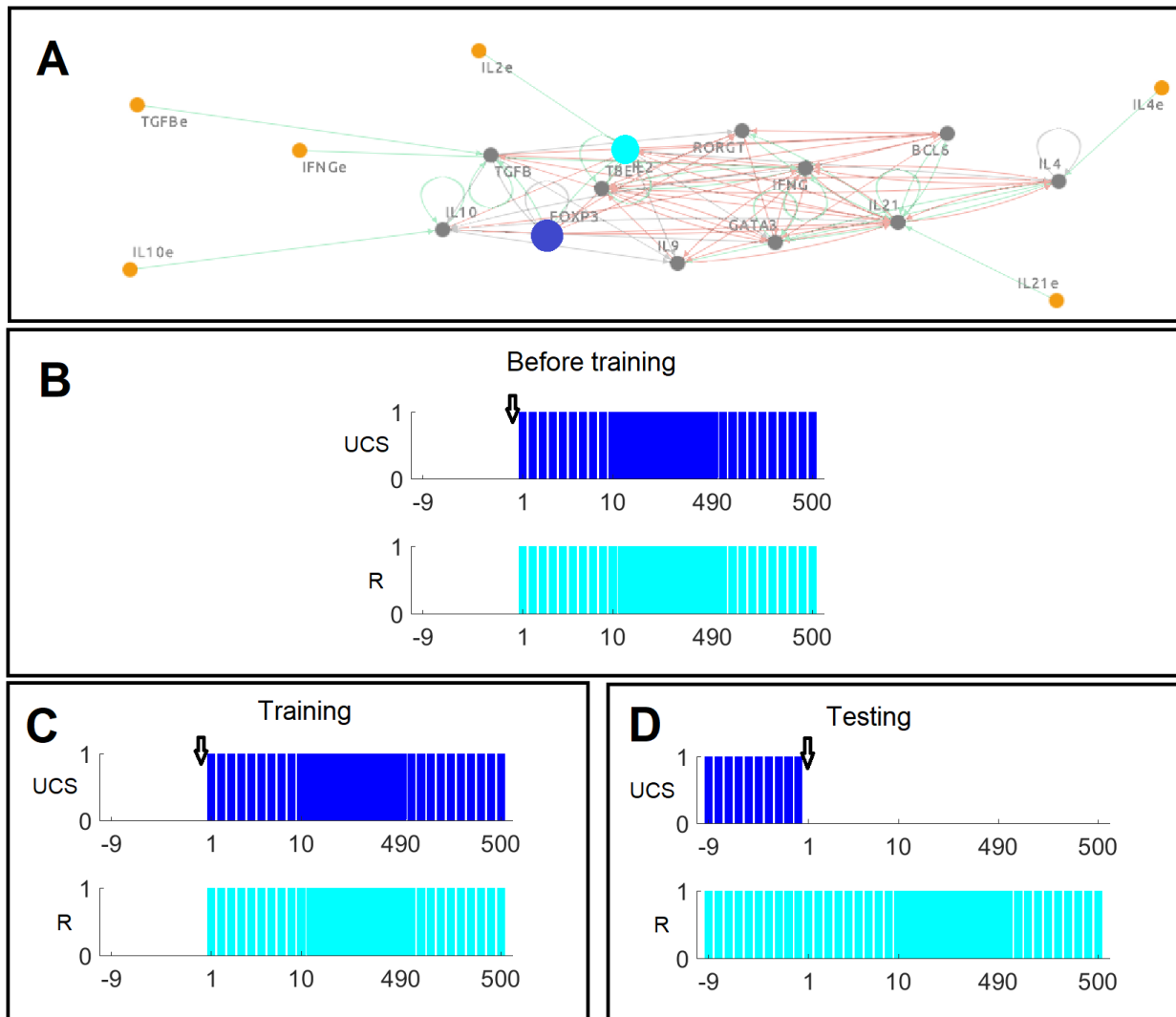
categories of AM, LRAM and SRAM, as individual memory types. (A) Input of a GRN with a R-UCS pair and a probable list of NS. (B) The memory detection process. At the top of the figure we define the different modules frequently used in the section B. The process works as follows. 1) choose a stimulus set; 2) flip the state of the stimuli and fix them in that state, referred to as clamping; 3) simulate the BN for M time-steps; 4) record the state of R compared to its state prior to the clamping step; 5) unclamp the stimuli (allow them to update states), referred to as relaxation; 6) simulate the BN for M time-steps; 7) record the state of R compared to its state prior to relaxation; 8) choose a different stimulus set; 9) flip and clamp the stimuli; 10) simulate the BN for M time-steps; 11) record the state of R compared to its state prior to the clamping step 9; 12) relax the network; and 13) record the state of R. We deem a given stimulus-response combination as having elicited a specific type of memory if it satisfies a number of specific conditions described fully in the Methods.

Supplemental Table 1: GRNs analyzed from cell collective [This item relates to Figure 3]

IDs	GRNs
#1	Arabidopsis thaliana Cell Cycle
#2	Aurora Kinase A in Neuroblastoma
#3	B cell differentiation
#4	BT474 Breast Cell Line Long-term ErbB Network
#5	BT474 Breast Cell Line Short-term ErbB Network
#6	Body Segmentation in Drosophila 2013
#7	Budding Yeast Cell Cycle
#8	Budding Yeast Cell Cycle 2009
#9	CD4+ T Cell Differentiation and Plasticity
#10	Cardiac development
#11	Cell Cycle Transcription by Coupled CDK and Network Oscillators
#12	Cortical Area Development
#13	FGF pathway of Drosophila Signaling Pathways
#14	Fanconi anemia and checkpoint recovery
#15	HCC1954 Breast Cell Line Long-term ErbB Network
#16	HCC1954 Breast Cell Line Short-term ErbB Network
#17	HH Pathway of Drosophila Signaling Pathways
#18	Human Gonadal Sex Determination
#19	Iron acquisition and oxidative stress response in aspergillus fumigatus
#20	Lac Operon
#21	Mammalian Cell Cycle
#22	Mammalian Cell Cycle 2006
#23	Metabolic Interactions in the Gut Microbiome
#24	Neurotransmitter Signaling Pathway
#25	Oxidative Stress Pathway
#26	Predicting Variabilities in Cardiac Gene
#27	Processing of Spz Network from the Drosophila Signaling Pathway
#28	Regulation of the L-arabinose operon of Escherichia coli
#29	SKBR3 Breast Cell Line Long-term ErbB Network
#30	SKBR3 Breast Cell Line Short-term ErbB Network
#31	T cell differentiation
#32	T-LGL Survival Network 2011 Reduced Network
#33	TOL Regulatory Network
#34	Toll Pathway of Drosophila Signaling Pathway
#35	VEGF Pathway of Drosophila Signaling Pathway

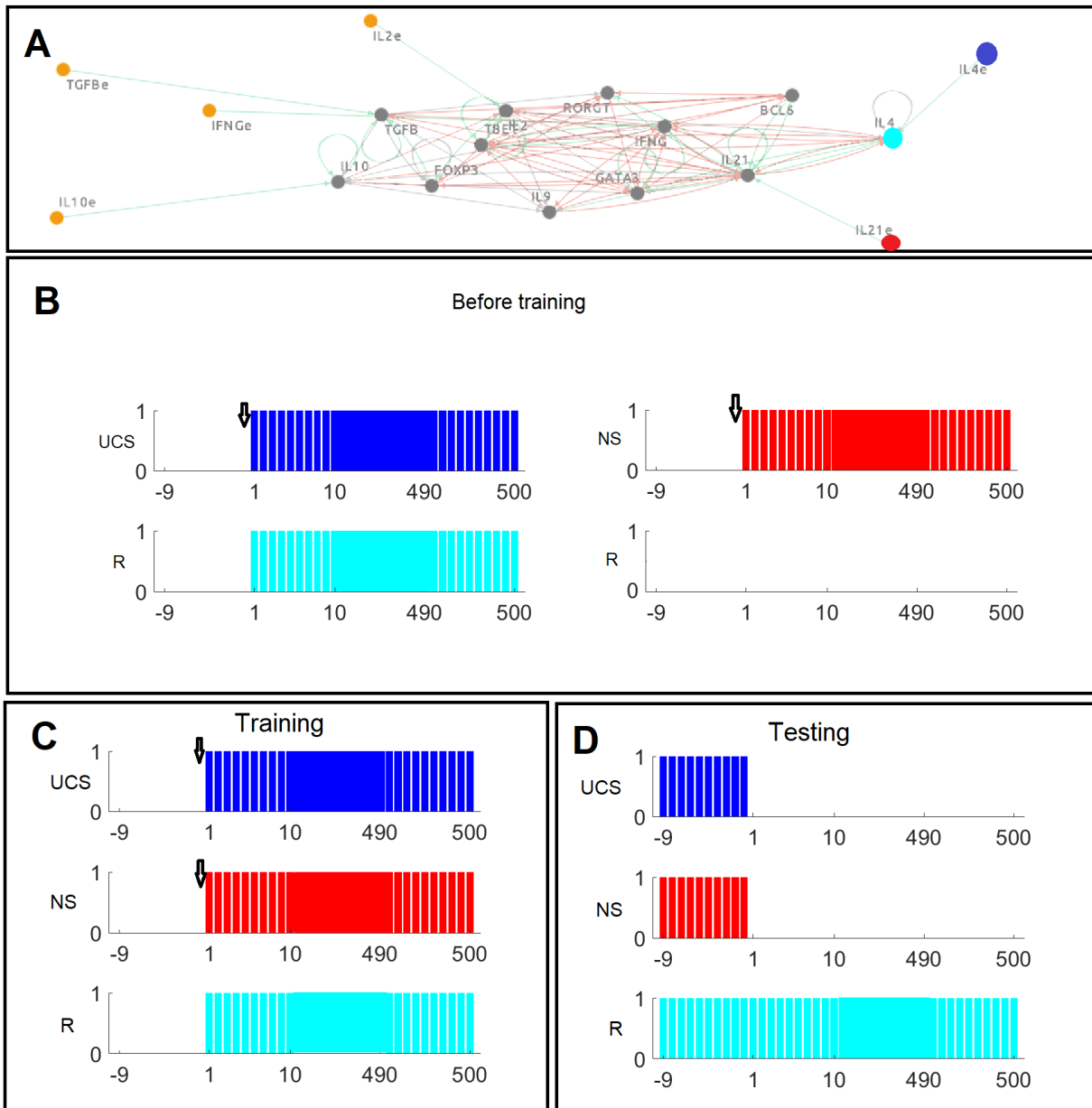
Legend: GRNs from Cell Collective that were analyzed, all having 25 or fewer nodes.

Supplemental Figure 3: Time series data from the evaluation of a sample UCS Based Memory [This item relates to Figure 4]



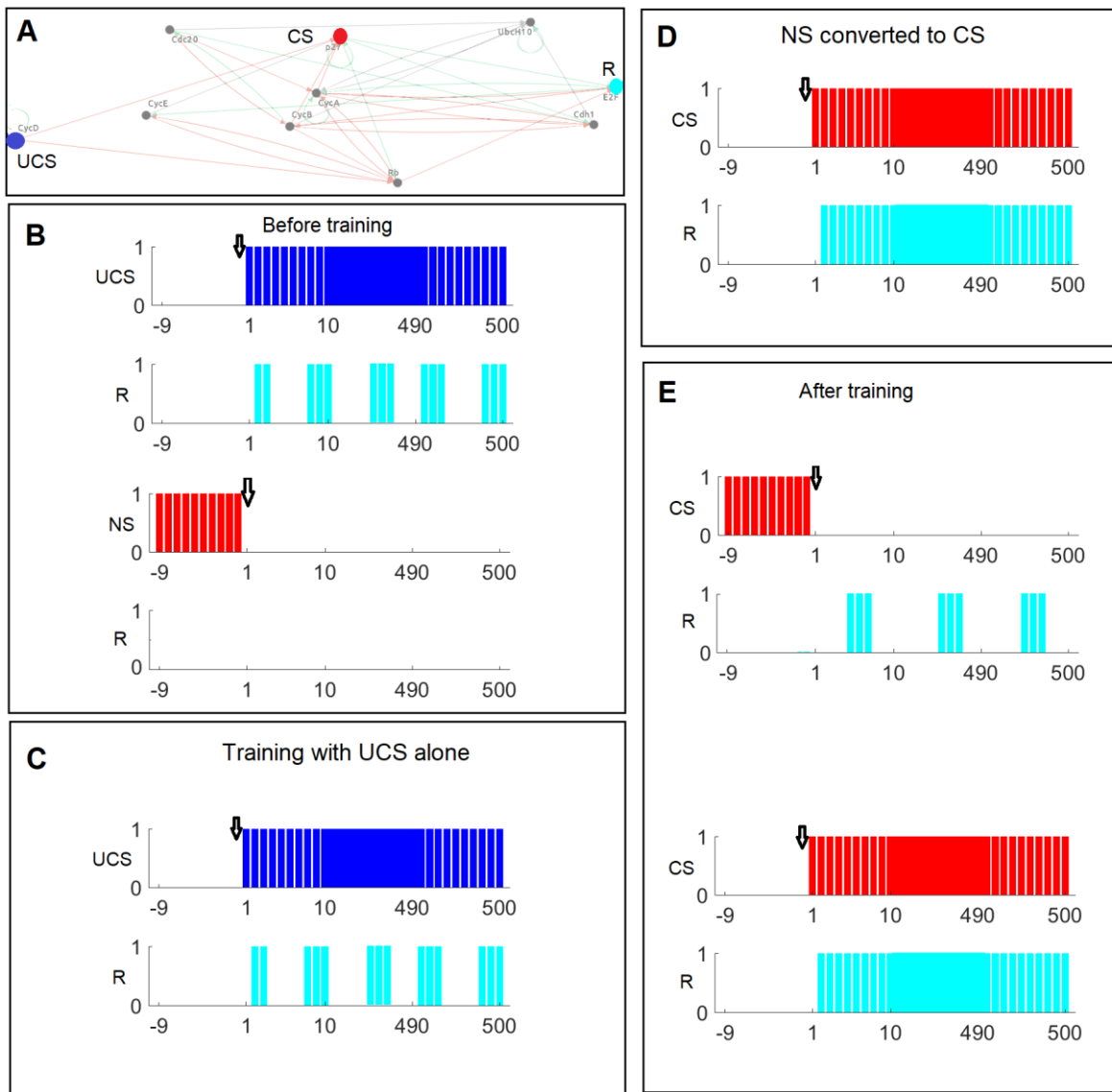
Legend: These node traces show the timeseries data for an example of UCS Based memory evaluation in the CD4+ T Cell Differentiation and Plasticity GRN. Here, the memory is established between FOXP3 gene as UCS and IL2 gene as response. A) The network with specified stimulus-response combination. B) The pre-requisite before learning that UCS has the capability of triggering R. C) The training of R by inducing UCS repeatedly. D) Testing of R making UCS off.

Supplemental Figure 4: Time series data from the evaluation of a sample Pairing Memory [This item relates to Figure 4]



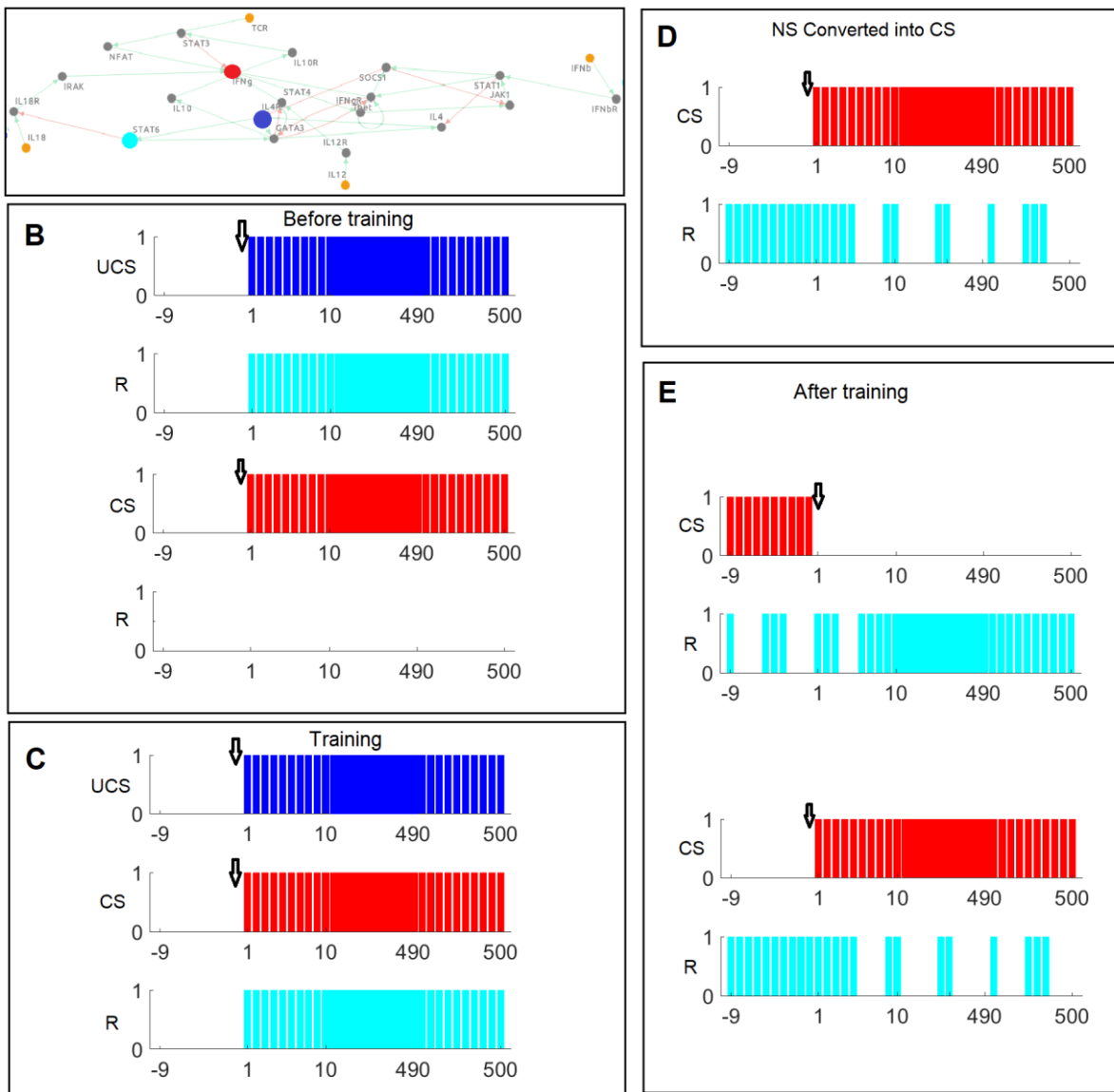
Legend: These node traces show the timeseries data for an example of Pairing memory evaluation in the CD4+ T Cell Differentiation and Plasticity GRN. Here, the memory is established among IL4e gene as UCS, IL2e as NS and IL4 gene as response. A) The network with specified stimulus-response combination. B) The pre-requisite before learning that UCS has the capability of triggering R and that NS should not trigger R. C) The training by inducing {UCS, NS} together repeatedly. D) testing of R making the stimuli off.

Supplemental Figure 5: Time series data from an evaluation of a sample Transfer Memory [This item relates to Figure 4]



Legend: These node traces show the timeseries data for an example the evaluation of Transfer memory in Mammalian Cell Cycle 2006 GRN. Here, the memory is established among CycD gene as UCS, P27 as NS/CS and E2F gene as response. A) The network with specified stimulus-response combination. B) The pre-requisite before learning that UCS has the capability of triggering R and that NS should not trigger R. C) The training by inducing {UCS, NS} together repeatedly. D) Testing of R to check if NS has converted to CS through training. Here, when the CS was turned off after learning, the R is not totally off but exhibits some ripples; during the on phase of CS response of R is consistent. E) As further confirmation of stable causality established between CS and R by training, we first deactivated CS, to see R get deactivated, and then reactivated the CS to ensure that it can activate R again.

Supplemental Figure 6: Time series data from the evaluation of a sample Consolidation Memory [This item relates to Figure 4]



Legend: These node traces show the timeseries data for a Consolidation memory in T cell differentiation GRN. Here, the memory is established among IL4R gene as UCS, IFNG as NS/CS and STAT6 gene as response. A) The network with specified stimulus-response combination. B) The pre-requisite of learning, stated as before learning shows that UCS has the capability of triggering R and that NS should not trigger R. C) Shows The training by inducing {UCS, NS} together repeatedly and D) testing that NS is converted to CS, i.e. it alone can induce R. Here, CS has an inverse relation with R, i.e. when CS is on makes R off and when CS goes off triggers R. The CS being on does not make R totally off but exhibits some ripples in R. But when CS is off, R lately becomes fully ON.

E) As further confirmation of stable causality established between CS and R by training, we first deactivate CS, to see R get deactivated, and then reactivated the CS to ensure that it can activate R again.

Data S1: Set of Boolean Expressions for each of the GRNs. [This item relates to Figure 3]

Legend: See file Expressions.zip – This file provides Boolean equations required to simulate each of the 35 GRNs used here from Cell Collective database (<https://cellcollective.org/>). The equation associated with a gene of a GRN comprises its regulators related by Boolean operators like AND, OR and NOT. We evaluate the equation during GRN simulation and assigns the result as the state of the current gene. We assign 0 to an external component during simulation.

Supplemental Table 2: Memory Evaluation of GRNs [This item relates to Figure 7]

UM	PM	TM	AM	LRAM	SRAM	CM	NM
0.00	0.00	0.00	0.00	0.00	0.00	0.00	100.00
29.79	0.51	6.98	2.64	2.47	0.17	0.00	60.09
46.82	0.74	11.12	0.11	0.11	0.00	0.00	41.21
95.25	0.00	4.75	0.00	0.00	0.00	0.00	0.00
96.02	0.00	3.98	0.00	0.00	0.00	0.00	0.00
0.00	0.00	0.00	0.00	0.00	0.00	0.00	100.00
0.00	0.00	0.00	0.00	0.00	0.00	0.00	100.00
0.00	0.00	0.00	0.00	0.00	0.00	0.00	100.00
59.94	2.21	29.02	0.95	0.95	0.00	0.00	7.89
47.58	0.00	3.86	0.00	0.00	0.00	0.00	48.55
0.00	0.00	0.00	2.33	2.33	0.00	0.00	97.67
42.11	0.00	21.05	0.00	0.00	0.00	0.00	36.84
0.00	0.00	0.00	0.00	0.00	0.00	0.00	100.00
0.00	0.00	0.00	0.00	0.00	0.00	2.84	97.16
95.22	0.00	4.78	0.00	0.00	0.00	0.00	0.00
90.76	0.00	9.24	0.00	0.00	0.00	0.00	0.00
0.00	0.00	0.00	0.00	0.00	0.00	0.00	100.00
81.19	0.30	16.45	0.00	0.00	0.00	0.00	2.06
0.00	0.00	0.00	0.00	0.00	0.00	0.00	100.00
0.00	0.00	0.00	0.00	0.00	0.00	0.00	100.00
76.63	0.00	10.02	0.00	0.00	0.00	0.00	13.36
12.04	0.00	4.63	2.78	0.93	1.85	0.00	80.56

80.41	0.00	9.28	0.00	0.00	0.00	0.00	10.31
0.00	1.16	0.58	1.16	1.16	0.00	0.00	97.09
0.00	0.00	0.00	0.00	0.00	0.00	0.00	100.00
47.58	0.00	3.86	0.00	0.00	0.00	0.00	48.55
0.00	0.00	0.00	0.00	0.00	0.00	0.00	100.00
0.00	0.00	0.00	0.00	0.00	0.00	0.00	100.00
93.20	0.00	6.80	0.00	0.00	0.00	0.00	0.00
97.60	0.00	2.40	0.00	0.00	0.00	0.00	0.00
64.48	0.00	15.51	0.00	0.00	0.00	0.07	19.94
93.71	0.00	0.00	0.00	0.00	0.00	0.00	6.29
0.00	0.00	0.00	0.00	0.00	0.00	0.00	100.00
0.00	0.00	0.00	0.00	0.00	0.00	0.00	100.00
0.00	0.00	0.00	0.00	0.00	0.00	0.00	100.00

Legend: For each GRN, the proportion of each memory type out of the total memory (within the available feasible combinations) has been calculated and put in the table. For those networks where no feasible combinations of stimulus/response were available, the proportion of no memory (NM) was considered as 100%.

Supplemental Table 3: p-value Test: comparing incidence of memories within GRNs vs. RBNs. [This item relates to Figure 8]

GRNs	UM	PM	TM	AM	LRAM	SRAM	CM	NM
#1	0.85	0.99	0.96	1	1	1	0.99	0.85
#2	0.1	0.15	0.08	0.03	0.03	0.09	0.7	0.08
#3	0.02	0.12	0.06	0.76	0.81	0.9	0.7	0.03
#4	0	0.8	0.15	0.73	0.81	0.86	0.58	0
#5	0	0.86	0.11	0.84	0.89	0.93	0.88	0
#6	0.62	0.86	0.74	0.84	0.89	0.93	0.88	0.52
#7	0.57	0.81	0.58	0.76	0.81	0.9	0.7	0.33
#8	0.62	0.86	0.74	0.84	0.89	0.93	0.88	0.52
#9	0.02	0.03	0	0.1	0.05	0.93	0.88	0
#10	0.05	0.86	0.11	0.84	0.89	0.93	0.88	0.06
#11	0.92	1	0.98	0	0	1	1	0.92
#12	0.06	1	0.02	1	1	1	1	0.06
#13	0.57	0.81	0.58	0.76	0.81	0.9	0.7	0.33
#14	0.62	0.86	0.74	0.84	0.89	0.93	0.03	0.58
#15	0	0.8	0.15	0.73	0.81	0.86	0.58	0
#16	0	0.86	0.02	0.84	0.89	0.93	0.88	0
#17	0.57	0.81	0.58	0.76	0.81	0.9	0.7	0.33
#18	0	0.14	0.01	0.84	0.89	0.93	0.88	0
#19	0.57	0.81	0.58	0.76	0.81	0.9	0.7	0.33
#20	0.85	0.99	0.96	1	1	1	0.99	0.85
#21	0	0.81	0.07	0.76	0.81	0.9	0.7	0.01
#22	0.13	0.99	0	0	0	0	0.99	0.1
#23	0	0.99	0	1	1	1	0.99	0
#24	0.62	0.04	0.74	0.07	0.04	0.93	0.88	0.58
#25	0.62	0.86	0.74	0.84	0.89	0.93	0.88	0.52
#26	0.05	0.86	0.11	0.84	0.89	0.93	0.88	0.06
#27	0.57	0.81	0.58	0.76	0.81	0.9	0.7	0.33
#28	0.85	0.99	0.96	1	1	1	0.99	0.85
#29	0	0.8	0.1	0.73	0.81	0.86	0.58	0
#30	0	0.86	0.2	0.84	0.89	0.93	0.88	0
#31	0	0.81	0.03	0.76	0.81	0.9	0.7	0.01
#32	0	0.86	0.74	0.84	0.89	0.93	0.88	0
#33	0.57	0.81	0.58	0.76	0.81	0.9	0.7	0.33
#34	0.85	0.99	0.96	1	1	1	0.99	0.85
#35	0.62	0.86	0.74	0.84	0.89	0.93	0.88	0.52
(%)	37.142	5.714	20	5.571	11.428	2.857	2.857	37.142

Legend: For each GRN, we calculated a p-value for the position of the incidence of each type of memory within the probability distribution of 100 similar size RBNs. If the p-value

is less than or equal to 0.05, the statistical test rejects the null hypothesis that the incidence of that type of memory in the GRN is not an outlier amongst similar sized RBN memories.

Supplemental Table 4: Outlier Test: comparing incidence of memories within GRNs vs. RBNs. [This item relates to Figure 8]

GRNs	UM	PM	TM	AM	LRAM	SRAM	CM	NM
#1	0	0	0	0	0	0	0	0
#2	0	0	0	1	1	0	0	0
#3	1	0	0	0	0	0	0	1
#4	1	0	0	0	0	0	0	1
#5	1	0	0	0	0	0	0	1
#6	0	0	0	0	0	0	0	0
#7	0	0	0	0	0	0	0	0
#8	0	0	0	0	0	0	0	0
#9	1	1	1	0	0	0	0	1
#10	0	0	0	0	0	0	0	0
#11	0	0	0	1	1	0	0	0
#12	0	0	1	0	0	0	0	0
#13	0	0	0	0	0	0	0	0
#14	0	0	0	0	0	0	1	0
#15	1	0	0	0	0	0	0	1
#16	1	0	1	0	0	0	0	1
#17	0	0	0	0	0	0	0	0
#18	1	0	1	0	0	0	0	1
#19	0	0	0	0	0	0	0	0
#20	0	0	0	0	0	0	0	0
#21	1	0	0	0	0	0	0	1
#22	0	0	1	1	1	1	0	0
#23	1	0	1	0	0	0	0	1
#24	0	1	0	0	1	0	0	0
#25	0	0	0	0	0	0	0	0
#26	0	0	0	0	0	0	0	0
#27	0	0	0	0	0	0	0	0
#28	0	0	0	0	0	0	0	0
#29	1	0	0	0	0	0	0	1
#30	1	0	0	0	0	0	0	1
#31	1	0	1	0	0	0	0	1
#32	1	0	0	0	0	0	0	1
#33	0	0	0	0	0	0	0	0
#34	0	0	0	0	0	0	0	0
#35	0	0	0	0	0	0	0	0
# Outlier	13	2	7	3	4	1	1	13
(%)	37.142	5.714	20	5.571	11.428	2.857	2.857	37.142

Legend: We tested whether the incidence of each type of memory of a GRN is an outlier in the pool of similar size of 100 RBNs: '1' if outlier; '0' otherwise. The last two rows show total number and percentage of outliers in each memory type.

Supplemental Table 5: p-value Test: comparing memories in GRNs vs. in Configuration models [This item relates to Figure 9]

GRNs	UM	PM	TM	AM	LRAM	SRAM	CM	NM
#1	0.7	0.92	0.74	0.89	0.94	0.92	0.79	0.55
#2	0.05	0.05	0.03	0.01	0.01	0.04	0.89	0.03
#3	0.03	0.02	0.01	0.04	0.04	1	0.93	0.02
#4	0	0.92	0.05	0.91	0.93	0.98	0.93	0
#5	0	0.95	0.11	0.97	0.97	1	0.96	0
#6	0.76	0.9	0.78	0.91	0.92	0.99	0.96	0.68
#7	0.76	0.9	0.74	0.92	0.93	0.99	0.94	0.68
#8	0.62	0.81	0.6	0.86	0.89	0.95	0.84	0.46
#9	0	0	0	0	0	1	0.94	0
#10	0.11	0.83	0.2	0.85	0.87	0.97	0.84	0.13
#11	0.7	0.9	0.71	0.08	0.07	0.98	0.94	0.6
#12	0.19	0.98	0.1	0.98	0.98	1	0.99	0.19
#13	0.85	0.96	0.93	0.97	0.97	1	1	0.83
#14	0.73	0.89	0.7	0.92	0.93	0.99	0.04	0.64
#15	0	0.92	0.08	0.92	0.93	0.98	0.91	0
#16	0	0.95	0.06	0.95	0.95	1	0.95	0
#17	0.94	0.99	0.94	0.99	1	0.99	1	0.93
#18	0	0.13	0.03	0.81	0.85	0.93	0.72	0
#19	0.64	0.87	0.62	0.86	0.88	0.97	0.93	0.52
#20	0.75	0.96	0.78	0.93	0.95	0.98	0.98	0.68
#21	0	0.87	0.08	0.85	0.89	0.94	0.82	0
#22	0.25	0.9	0.25	0.07	0.1	0.01	0.89	0.24
#23	0	0.94	0.1	0.94	0.94	1	0.96	0
#24	0.6	0.11	0.68	0.17	0.12	0.92	0.85	0.45
#25	0.67	0.92	0.71	0.91	0.93	0.98	0.87	0.54
#26	0.05	0.89	0.16	0.88	0.9	0.96	0.9	0.06
#27	0.74	0.97	0.85	0.94	0.95	0.99	0.96	0.69
#28	0.83	0.97	0.83	0.97	0.98	0.99	0.97	0.79
#29	0	0.89	0.03	0.9	0.9	0.97	0.89	0
#30	0	0.96	0.11	0.96	0.96	1	0.99	0
#31	0	0.88	0	0.87	0.88	0.98	0.06	0
#32	0	0.81	0.6	0.78	0.8	0.93	0.7	0.01
#33	0.82	0.98	0.87	0.98	0.98	1	0.97	0.78
#34	0.69	0.96	0.88	0.97	0.97	1	0.98	0.64
#35	0.86	0.98	0.91	0.98	0.98	1	0.98	0.83
(%)	37.143	5.714	17.14	8.571	8.571	5.714	2.857	40

Legend: For each GRN, the stated p-value represents the incidence of each memory type fit into the probability distribution of its random ensemble. If the p-value is less than

or equal to 0.05, the statistical test rejected the null hypothesis that the amount of the memory in the GRN is not an outlier in its random ensemble.

Supplemental Table 6: Outlier Test: comparing memory incidence in GRNs vs. Configuration models [This item relates to Figure 9]

GRNs	UM	PM	TM	AM	LRAM	SRAM	CM	NM
#1	0	0	0	0	0	0	0	0
#2	0	0	1	1	1	1	0	1
#3	1	1	1	1	1	0	0	1
#4	1	0	0	0	0	0	0	1
#5	1	0	0	0	0	0	0	1
#6	0	0	0	0	0	0	0	0
#7	0	0	0	0	0	0	0	0
#8	0	0	0	0	0	0	0	0
#9	1	1	1	1	1	0	0	1
#10	0	0	0	0	0	0	0	0
#11	0	0	0	0	0	0	0	0
#12	0	0	0	0	0	0	0	0
#13	0	0	0	0	0	0	0	0
#14	0	0	0	0	0	0	1	0
#15	1	0	0	0	0	0	0	1
#16	1	0	0	0	0	0	0	1
#17	0	0	0	0	0	0	0	0
#18	1	0	1	0	0	0	0	1
#19	0	0	0	0	0	0	0	0
#20	0	0	0	0	0	0	0	0
#21	1	0	0	0	0	0	0	1
#22	0	0	0	0	0	1	0	0
#23	1	0	0	0	0	0	0	1
#24	0	0	0	0	0	0	0	0
#25	0	0	0	0	0	0	0	0
#26	0	0	0	0	0	0	0	0
#27	0	0	0	0	0	0	0	0
#28	0	0	0	0	0	0	0	0
#29	1	0	1	0	0	0	0	1
#30	1	0	0	0	0	0	0	1
#31	1	0	1	0	0	0	0	1
#32	1	0	0	0	0	0	0	1
#33	0	0	0	0	0	0	0	0
#34	0	0	0	0	0	0	0	0
#35	0	0	0	0	0	0	0	0
#Outlier	13	2	6	3	3	2	1	14
(%)	37.143	5.714	17.14	8.571	8.571	5.714	2.857	40

Legend: We tested whether the incidence of a certain memory type of a GRN is an outlier in its random ensemble (corresponding values of 100 configuration models of the GRN). ‘1’ if outlier; ‘0’ otherwise. The last two rows show the total number and percentage of outlier in each memory type.

Supplemental Table 7: The distribution of the transient length of RBNs. [This item relates to Figure 8]

N	Median	Mean	99%	Max
10	3	3.414	12.01	29
15	11	13.648	53.01	104
20	14	19.302	86.02	142
25	77	113.639	494.18	1180
30	122	192.661	1070.54	2572
35	1605	2558.796	14593.67	36478
40	3918	6755.941	42507.43	78016

Legend: The distribution of the transient length of RBNs. This table shows transient length data obtained from simulations of 1000 RBNs for each N (number of nodes), with each RBN run 1000 times starting from a different initial condition each time. Here, transient length indicates the number of time steps taken by a Boolean network to reach an attractor from a given initial state.

Supplemental Table 8: Edge densities of biological GRNs. [This item relates to Figure 7]

GRNs	Number of Nodes	Number of Edges	Edge Density
Arabidopsis thaliana Cell Cycle	14	66	33.673
Aurora Kinase A in Neuroblastoma	23	43	8.129
B cell differentiation	22	39	8.058
BT474 Breast Cell Line Long-term ErbB Network	25	70	11.200
BT474 Breast Cell Line Short-term ErbB Network	16	46	17.969
Body Segmentation in Drosophila 2013	17	29	10.035
Budding Yeast Cell Cycle	20	42	10.500
Budding Yeast Cell Cycle 2009	18	59	18.210

CD4+ T Cell Differentiation and Plasticity	18	78	24.074
Cardiac development	15	38	16.889
Cell Cycle Transcription by Coupled CDK and Network Oscillators	9	19	23.457
Cortical Area Development	5	14	56.000
FGF pathway of Drosophila Signalling Pathways	23	24	4.537
Fanconi anemia and checkpoint recovery	15	66	29.333
HCC1954 Breast Cell Line Long-term ErbB Network	25	70	11.200
HCC1954 Breast Cell Line Short-term ErbB Network	16	46	17.969
HH Pathway of Drosophila Signaling Pathways	24	32	5.556
Human Gonadal Sex Determination	19	79	21.884
Iron acquisition and oxidative stress response in aspergillus fumigatus	22	38	7.851
Lac Operon	13	22	13.018
Mammalian Cell Cycle	20	51	12.750
Mammalian Cell Cycle 2006	10	35	35.000
Metabolic Interactions in the Gut Microbiome	12	30	20.833
Neurotransmitter Signaling Pathway	16	22	8.594
Oxidative Stress Pathway	19	32	8.864
Predicting Variabilities in Cardiac Gene	15	38	16.889
Processing of Spz Network from the Drosophila Signaling Pathway	24	28	4.861
Regulation of the L-arabinose operon of Escherichia coli	13	17	10.059
SKBR3 Breast Cell Line Long-term ErbB Network	25	81	12.960
SKBR3 Breast Cell Line Short-term ErbB Network	16	41	16.016
T cell differentiation	23	34	6.427
T-LGL Survival Network 2011 Reduced Network	18	43	13.272
TOL Regulatory Network	24	48	8.333
Toll Pathway of Drosophila Signaling Pathway	11	11	9.091
VEGF Pathway of Drosophila Signaling Pathway	18	18	5.556
Average edge density (%)			15.401

Legend: For each biological GRN that we analyzed, we show here the number of edges they contain, the edge density (calculated as the proportion of the number of actual edges with respect to the number of possible edges which is simply $(Number\ of\ Nodes)^2$). The average edge density of around 13% was used as a basis for the choice of the edge density (10%) for the RBNs that we simulated.

Supplemental Table 9. The distribution of the constancy length of RBNs. [This item relates to Figure 8]

N	Median	Mean	95%	99%	Max
10	1	1.709313	4	8	31
15	2	2.553708	7	13	183
20	2	3.056888	8	18	94
25	3	4.872672	13	32	489
30	4	6.44254	18	51	1195
35	8	17.08245	29	167.46	8598
40	10	31.6757	36	397	27908

Legend: This table shows constancy length data obtained from simulations of 1000 RBNs for each N (number of nodes), with each RBN run 1000 times starting from a different initial condition each time. Here, constancy length indicates the maximum number of contiguous steps during which a node preserves its state (0 or 1) in an attractor, taken as the maximum over all nodes. For example, consider a network with N>2 nodes, of which node 'X' goes through the following states in an attractor cycle (period length of 13 steps) in the same order: 0110001001111, and node 'Y' goes through the following states in the same order: 0110000001111. Here, the constancy length of 'X' is 4 and that of 'Y' is 6. The constancy length of the network would be the maximum of the constancy lengths of the individual nodes.

Data S2: See file Violins.zip – plots comparing distribution of memories for GRNs to their randomized configuration models. [This item relates to Figure 9]

Legend: This supplement provides the violin plots of the set of all 35 GRNs (Plot 1-35) from the Cell Collective database (<https://cellcollective.org/>) compared (in terms of memories) to their configuration models. We show the mean (black line), median (red line), 5th percentile (teal line) and 95th percentile (pink line). The actual frequency of memory of the real GRN is represented as a red star. We calculated the conditional entropy among the different types of memories of GRNs and Configuration models, normalized these conditional entropies, applied Gaussian smoothing and visualized the results obtained.

References Cited

- Graudenzi, A., Serra, R., Villani, M., Colacci, A., and Kauffman, S.A. (2011). Robustness analysis of a Boolean model of gene regulatory network with memory. *Journal of Computational Biology* 18, 559-577.
- Groß, A., Kracher, B., Kraus, J.M., Kühlwein, S.D., Pfister, A.S., Wiese, S., Luckert, K., Pötz, O., Joos, T., and Van Daele, D. (2019). Representing dynamic biological networks with multi-scale probabilistic models. *Communications biology* 2, 1-12.
- Helikar, T., Kowal, B., McClenathan, S., Bruckner, M., Rowley, T., Madrahimov, A., Wicks, B., Shrestha, M., Limbu, K., and Rogers, J.A. (2012). The cell collective: toward an open and collaborative approach to systems biology. *BMC systems biology* 6, 96.
- Herrmann, F., Gross, A., Zhou, D., Kestler, H.A., and Kuhl, M. (2012). A boolean model of the cardiac gene regulatory network determining first and second heart field identity. *PLoS One* 7, e46798.
- Kauffman, S., Peterson, C., Samuelsson, B.r., and Troein, C. (2003). Random Boolean network models and the yeast transcriptional network. *PNAS* 100.
- Mochizuki, A., Fiedler, B., Kurosawa, G., and Saito, D. (2013). Dynamics and control at feedback vertex sets. II: A faithful monitor to determine the diversity of molecular activities in regulatory networks. *Journal of theoretical biology* 335, 130-146.
- Naldi, A., Hernandez, C., Levy, N., Stoll, G., Monteiro, P.T., Chaouiya, C., Helikar, T., Zinovyev, A., Calzone, L., and Cohen-Boulakia, S. (2018). The CoLoMoTo interactive notebook: accessible and reproducible computational analyses for qualitative biological networks. *Frontiers in physiology* 9, 680.
- Serra, R., d, M.V., Damiania, C., Graudenzi, A., Colaccib, A., and Kauffmanc, S.A. (2007). Interacting Random Boolean Networks. *Proceedings of ECCS07: European Conference on Complex Systems*.
- Shmulevich, I., and Dougherty, E.R. (2010). Probabilistic Boolean networks: the modeling and control of gene regulatory networks (SIAM).
- Shmulevich, I., and Kauffman, S.A. (2004). Activities and sensitivities in boolean network models. *Phys Rev Lett* 93, 048701.
- Veliz-Cuba, A., Aguilar, B., Hinkelmann, F., and Laubenbacher, R. (2014). Steady state analysis of Boolean molecular network models via model reduction and computational algebra. *BMC Bioinformatics*.
- Xiao, Y. (2009). A Tutorial on Analysis and Simulation of Boolean Gene Regulatory Network Models. *Current Genomics* 10, 511-525.
- Zhai, X., Zhou, W., Fei, G., Liu, W., Xu, Z., Jiao, C., Lu, C., and Hu, G. (2018). Null model and community structure in multiplex networks. *Scientific reports* 8, 1-13.